

1 **Seasonal streamflow forecasts for Europe – I. Hindcast verification**
2 **with pseudo- and real observations**

3

4 Wouter Greuell¹⁾, Wietse H. P. Franssen¹⁾, Hester Biemans²⁾ and Ronald W. A.
5 Hutjes^{1,2)}

6

7 1) Water Systems and Global Change, Wageningen University,
8 Droevendaalsesteeg 3, NL 6708 PB Wageningen, Netherlands

9 2) Water and Food, Wageningen Environmental Research, Droevendaalsesteeg 3,
10 NL 6708 PB Wageningen, Netherlands

11

12 correspondence to wouter.greuell@wur.nl

13

14

15 **Abstract**

16

17 Seasonal predictions of river flow can be exploited among others to optimize
18 hydropower energy generation, navigability of rivers and irrigation management to
19 decrease crop yield losses. This paper is the first of two papers dealing with a physical
20 model-based system built to produce probabilistic seasonal hydrological forecasts,
21 applied here to Europe. This paper presents the development of the system and the
22 evaluation of its skill. The Variable Infiltration Capacity (VIC) hydrological model is
23 forced with bias-corrected output of ECMWF's Seasonal Forecasting System 4. For the
24 assessment of skill, we analysed hindcasts (1981-2010) against a reference run, in which
25 VIC was forced by gridded meteorological observations. The reference run was also
26 used to generate initial hydrological conditions for the hindcasts.

27 The skill in runoff and discharge hindcasts is analysed with monthly temporal
28 resolution, up to 7 months of lead time, for the entire annual cycle. Using the reference
29 run output as pseudo-observations and taking the correlation coefficient as metric, hot
30 spots of significant theoretical skill in discharge and runoff were identified in
31 Fennoscandia (from January to October), the southern part of the Mediterranean (from
32 June to August), Poland, northern Germany, Romania and Bulgaria (mainly from
33 November to January), western France (from December to May) and the eastern side of
34 Great Britain (January to April). Generally, the skill decreases with increasing lead time,
35 except in spring in regions with snow-rich winters. In some areas some skill persists
36 even at the longest lead times (7 months).

37 Theoretical skill was compared to actual skill as determined with real discharge
38 observations from 747 stations. Actual skill is generally substantially less than
39 theoretical skill. This effect is stronger for small than for large basins. Qualitatively, the
40 use of different skill metrics (correlation coefficient, ROC area and Ranked Probability
41 Skill Score) leads to broadly similar spatio-temporal patterns of skill, but the level of
42 skill decreases, and the area of skill shrinks, in the following order: correlation
43 coefficient, ROC area below normal tercile, ROC area above normal tercile, Ranked
44 Probability Skill Score and finally, ROC near normal tercile.

45

46

47

48 **1 Introduction**

49

50 Society may benefit from seasonal hydrological forecasts, i.e. hydrological forecasts for
51 future time periods from more than two weeks up to about a year (Doblas-Reyes et al.,
52 2013). Such predictions can e.g. be exploited to optimize hydropower energy generation
53 (Hamlet et al. 2002), navigability of rivers in low flow conditions (Li, et al., 2008) and
54 irrigation management (Ghile and Schulze 2008; Mushtaq et al. 2012) to decrease crop
55 yield losses. In order to be of any value in decision making processes in such sectors,
56 forecasts must be credible, i.e. be skilful in predicting anomalous system states, as well
57 as being relevant and legitimate to the decision making process (e.g. Bruno Soares and
58 Dessai, 2016). In this paper we will introduce WUSHP (Wageningen University
59 Seamless Hydrological Prediction system), a dynamical, model-based system (see Yuan
60 et al., 2015) that was built around the Variable Infiltration Capacity (VIC) hydrological
61 model and ECMWF's Seasonal Forecast System 4, to produce seasonal hydrological
62 forecasts. It will be applied to Europe. The usefulness of the system depends partially
63 on the level of its skill and the paper will therefore focus on an extensive assessment of
64 the skill of WUSHP. The usual method of assessing skill of predictive systems is by
65 analysing hindcasts, a strategy that will be adopted here as well.

66

67 During recent years, a number of systems for making seasonal hydrological forecasts
68 have been developed. Examples are the University of Washington's Surface Water
69 Monitor (SWM; Wood and Lettenmaier, 2006) and the African Drought Monitor
70 (Sheffield et al., 2014). Seasonal hydrological forecasting systems for the entire
71 continent of Europe are scarce (Bierkens and van Beek, 2009; Thober et al., 2015), but
72 a few more concentrate on smaller domains such as the British Isles (Svensson et al.,
73 2015), Iberia (Trigo, 2004) or France (Céron et al., 2010; Singla et al., 2012).

74

75 Thober et al. (2015) forced a mesoscale hydrological model (mHM) with meteorological
76 hindcasts from the North American Multi-Model Ensemble (NMME) to investigate the
77 predictability of soil moisture in continental Europe, excluding Fennoscandia.
78 Evaluating at seasonal resolution a number of forecasting techniques that produced
79 distinct variations in the magnitude of skill, they found that spatial patterns in skill were
80 remarkably similar among the different techniques, as well as comparable to the spatial
81 patterns of the autocorrelation (persistence) of reference soil moisture. High skill was
82 found in eastern Germany and Poland, Romania, the southern Balkans and eastern
83 Ukraine as well as north-western France. Less skill was found in the mountainous areas
84 of the Alps and the Pyrenees, the northern Adriatic and Atlantic Iberia. Most skill was
85 found for winter months (DJF), least for autumn (SON), this minimum shifting to
86 summer (JJA) at long lead times (6 months).

87

88 Bierkens and van Beek (2009) developed an analogue events method to select annual
89 ERA40 meteorological forcing on the basis of annual SST anomalies in the northern
90 Atlantic and then made hydrological forecasts with a global-scale hydrological model
91 applied to Europe. Evaluating only winter and summer half year aggregated skill for

92 discharge, they found wintertime skill in large parts of Europe with maxima in eastern
93 Spain and a zone from the southern Balkans and Romania through eastern Poland and
94 western Russia to the Baltic states and Finland. Summertime skill was lower, generally
95 by about 50% and even more around the Alps and the Adriatic. A climate forecast based
96 on the North Atlantic Oscillation (NAO) added significant skill only in limited areas,
97 such as Scandinavia, the Iberian Peninsula, the Balkans, and around the Black Sea.

98

99 Svensson et al. (2015) found skilful winter river flow forecasts across the whole of the
100 UK due to a combination of skilful winter rainfall forecasts for the north and west, and
101 strong persistence of initial hydrological conditions in the south and east. Strong
102 statistical correlations between the NAO index and winter precipitation in Iberia lead to
103 skilful forecasts of JFM river flow and hydropower production (Trigo et al., 2004).
104 Céron et al. (2010) and Singla et al. (2012) set up a high resolution river flow forecasting
105 system (8 km) over France, for which the seasonal climate forecast improved the MAM
106 skill over northern France, but worsened it over southern France (compared to a river
107 flow model with proper initialisation of soil moisture, snow etc., but random
108 atmospheric forcing). Demirel et al. (2015) found that both two physical models and
109 one neural network over-predict runoff during low-flow periods using ensemble
110 seasonal meteorological forcing for the Moselle basin. As a result forecasts of more
111 extreme low flows are less reliable than forecasts of more moderate ones.

112

113 It is quite common in seasonal hydrological forecasting (e.g. Shukla and Lettenmaier,
114 2011, Singla et al., 2012, Mo and Lettenmaier, 2014, and Thober et al., 2015) but also
115 in medium range forecasting (i.e. 14 days in Alfieri et al., 2014) to determine prediction
116 skill by comparing the hindcasts with the output from a reference simulation. A
117 reference simulation is a simulation made with the same hydrological model as the
118 hindcasts, except that the forcing is taken from meteorological observations or from a
119 gridded version of meteorological observations. The reference simulation can best be
120 regarded as a simulation that attempts to make a best estimate of the true conditions (in
121 terms of e.g. discharge, soil moisture and evapotranspiration), using the modelling
122 system. We will refer to the output of such a reference simulation as “pseudo-
123 observations” (alternatively named “true discharge” in Bierkens and Van Beek, 2009;
124 “synthetic truth” in Shukla and Lettenmaier, 2011; “reanalysis” in Singla et al., 2012;
125 “a posteriori estimates” in Shukla et al., 2014). We prefer the term “pseudo-
126 observations” over “re-analysis” since the latter has a meteorological connotation that
127 often implies the use of some form of (variational) data assimilation. We did not attempt
128 any form of assimilating observed hydrological variables, such as discharge, in our
129 reference run.

130

131 Pseudo-observations have the important advantages of being complete in the spatial and
132 the temporal domain and to be available for all model variables. Also, they are suitable
133 for the quantification of small sensitivities, e.g. to bias correction of the meteorological
134 forcing, which would be hard to detect with real observations. Finally, assessment of
135 skill based on pseudo-observations reduces model errors from the analysis to a

136 minimum, which is especially useful when addressing various sources of skill (Wood et
137 al., 2016), something we will do in the companion paper (Greuell et al., 2016, in
138 revision).

139

140 The downside of pseudo-observations is, of course, that they are not equal to real
141 observations. In this paper we will determine the performance of the prediction system
142 not only with pseudo-observations, but also with real observations of discharge (like
143 e.g. Koster et al., 2010, and Yuan et al., 2013) and compare the skill found with the two
144 different approaches (“theoretical and actual skill”, according to Van Dijk et al., 2013).
145 Such a comparison was previously made by Bierkens and Van Beek (2009) and Van
146 Dijk et al. (2013) and they found that theoretical skill generally exceeds actual skill.
147 This is in line with the fact that the pseudo-observations are obtained with the same
148 model as the hindcasts, which should logically lead to an overestimation of the skill
149 when the pseudo-observations are used for verification. We thus hypothesise that
150 theoretical skill exceeds actual skill. In this paper we will not only analyse the difference
151 between the skills obtained with the two different types of data but also discuss in some
152 detail conceptual differences between using pseudo- and real observations for
153 verification.

154

155 This paper aims to analyse to what extent WUSHP is able to predict runoff and discharge
156 in Europe over the full annual cycle and for lead times up to 7 months. We aim to assess
157 skill at monthly resolution instead of seasonal or semi-annual aggregates. Where many
158 studies use correlation coefficient as main skill metric we will also assess skill using
159 two probabilistic metrics, namely ROC area and RPSS (see Sect. 2.3). The second aim
160 of the paper is to get a better understanding of the effects of using pseudo-observations,
161 as opposed to using actual observations, for the verification of hindcasts. In the next
162 section we describe the concept and details of our modelling (Sect. 2.1) and analysis
163 approach (Sect. 2.2 and 2.3). We will start the result section by assessing theoretical
164 skill of the runoff hindcasts (Sect. 3.1) and then proceed to theoretical skill of the
165 discharge hindcasts and a comparison between theoretical skill of discharge and runoff
166 in Sect. 3.2. Differences between theoretical and actual skill of discharge will be
167 presented (Sect. 3.3) followed by an analysis of differences in skill determined with
168 various metrics in Sect. 3.4. The discussion starts with a conceptual analysis of reasons
169 for differences in actual and theoretical skill (Sect. 4.1), followed by a discussion of
170 uncertainties (Sect. 4.2) and implications (Sect. 4.3).

171

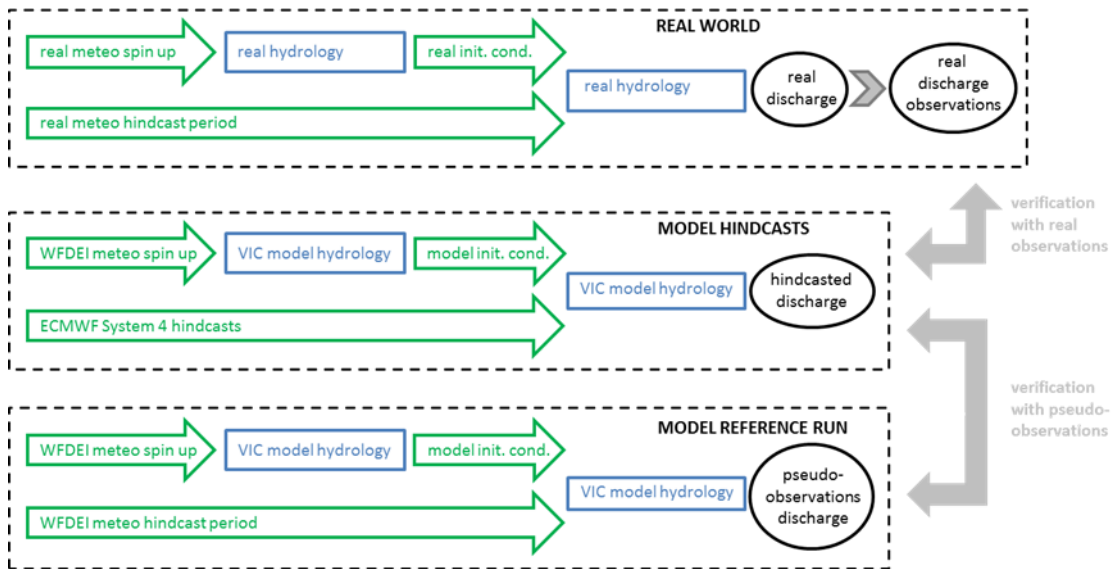
172 In a companion paper (Greuell et al., 2016) we analyse the reasons for the presence or
173 lack of skill discussed in the present paper, using two different methods. Firstly, skill in
174 the forcing and other directly related hydrological variables, like evapotranspiration, are
175 analysed. Secondly, a number of experiments similar to the conventional Ensemble
176 Streamflow Prediction (ESP) and reverse-ESP experiments, which isolate different
177 causes of predictability, are discussed. In the results and discussion sections of the
178 present paper we will occasionally look forward to the identified causes of skill.

179

180
181
182
183
184
185
186
187
188
189
190
191
192

2 System, models, data and methods of analysis

In the following subsections we will describe the various components of WUSHP (2.1), the real discharge observations (2.2) and the methods of analysis (2.3). Fig. 1 provides an outline of the system, which consists of the hindcasts themselves (middle box in the figure) and a model reference run (lower box). The hindcasts will be verified by means of the pseudo-observations, which are generated by the reference simulations, and by real discharge observations, which are “generated” in the real world (upper box). Differences between these two types of verifications will be discussed in Sect. 4.1.



193
194

Figure 1: Setup of the present study. The lower two dashed boxes summarise the setup of the forecast system itself. The upper dashed box represents the real world. The filled arrows on the right hand side represent verification of hindcasts (in the middle) with pseudo-observations (bottom) and with observations of real discharge (top). In each box the flow at the upper left represents the creation of initial conditions while the flow below that (a single arrow) represents the meteorological forcing.

202
203
204
205
206

2.1 The model, workflow and forcing data for the hindcasts and the reference simulation

207 WUSHP consists of two simulation branches: a single reference simulation (lower box
208 in Fig. 1) and the hindcasts themselves (middle box in same figure). In both branches,
209 terrestrial hydrology is simulated with the Variable Infiltration Capacity model (VIC,
210 see Liang et al., 1994), which runs on a domain extending from 25° W to 40° E and from

211 35° to 72° N, including 5200 land based cells of 0.5° x 0.5° (see maps in e.g. Fig. 2).
212 VIC is forced by a gridded data set of daily meteorological data (7 variables:
213 precipitation, minimum and maximum temperature, atmospheric humidity, wind speed
214 and incoming short- and long wave radiation).

215

216 In the reference simulation VIC is forced by the WATCH Forcing Data Era-Interim
217 (WFDEI; Weedon et al., 2014) for the period of 1979-2010, of which the first two years
218 were used to spin up the states of snow, soil moisture and discharge, and were not used
219 in further analysis. The reference simulation has the dual aim to create the pseudo-
220 observations for verification purposes (lower box in Fig. 1) and to create a best estimate
221 of the temporally varying model state, which is then used for the initialisation of the
222 hindcasts (flow from the upper left in the middle box of Fig. 1).

223

224 The second branch, the hindcasts, consists of three steps. Seasonal predictions of the
225 same set of 7 meteorological variables (see above) are taken from ECMWF's Seasonal
226 Forecast System 4 (S4 hereafter) at daily resolution. These are then bias-corrected using
227 WFDEI as the reference data set. Finally, VIC is run with the bias-corrected S4 hindcasts
228 as forcing, taking initial states from the reference simulation.

229

230 The S4 hindcasts used in the present study include 15 members, cover the period from
231 1981 to 2010 and consist of simulations with a duration of 7 months, starting and
232 initialised on the first day of every month (see Molteni et al., 2011 and the ECMWF
233 Seasonal Forecast User Guide, online). The S4 ensemble is constructed by combining a
234 5-member ensemble analysis of the ocean initial state with SST perturbations of that
235 state and with activation of stochastic physics.

236

237 All seven meteorological forcing variables were regridded with bi-linear interpolation
238 from the 0.75 x 0.75° lat-lon grid of the S4 hindcasts to a 0.5° x 0.5° grid. Since bias
239 correction generally improves forecasting skill, the quantile mapping method of
240 Themeßl et al. (2011) was applied to bias-correct the forcing variables, taking the
241 WFDEI as reference. For each variable and grid cell, 84 correction functions were
242 established and applied by separating the data according to target month (12) and lead
243 month (7). Such empirical distribution mapping of daily values has been successful in
244 improving especially forecast reliability (rather than sharpness and accuracy;
245 Crochemore et al., 2016).

246

247 VIC was run for the period of the S4 hindcasts (1981 – 2010). Additionally, for the
248 reference simulation two extra years (1979 – 1980) were simulated to spin up the states
249 of snow, soil moisture and discharge. The hindcast simulations were initialised with
250 states of soil moisture and snow from the reference simulation, so for these variables
251 spin up was not needed. However, due to the set-up of the routing module of VIC, the
252 state of discharge could not be saved and loaded. Hence to spin up discharge, each 7-
253 month hindcast simulation was preceded by one month simulation with WFDEI forcing.

254 Since the hindcasts cover 30 years with 12 initialisation dates each and consist of 15
255 members, a total of 5400 hindcast simulations was carried out.

256

257 VIC is run in so-called ‘energy balance mode’ which requires resolving the diurnal
258 cycle. Therefore, internally the model temporally disaggregates the daily input to 3-
259 hourly data and runs with a time step of 3 hours. The output of all variables is again at
260 a daily resolution. Because snow may contribute significantly to the seasonal
261 predictability of other hydrological variables, VIC was run with the option of subgrid
262 elevation bands. This means that for each grid cell calculations were carried out at up to
263 16 different elevations, with the aim of simulating the elevation gradient of snow. VIC
264 was run in naturalised flow mode, i.e. river regulation, irrigation and other
265 anthropogenic influences were not considered.

266

267 Simulations of historic discharge made with VIC (and four other hydrological models)
268 were validated with observations from large European rivers by Greuell et al. (2015)
269 and Roudier et al. (2016). VIC exhibits a fairly small average bias (across 46 stations)
270 of +23 mm/yr (= 7%) and overall differentiates well between low and high specific
271 discharge basins with a spatial correlation coefficient of 0.955. However, specific
272 discharge is overestimated in the Mediterranean and underestimated in northern
273 Fennoscandia. Annual cycles are fairly well reproduced across Europe, though VIC
274 somewhat overestimates their amplitude. In northern Fennoscandia the spring peak is
275 too late and lasts too long. Annual cycles are best reproduced for rain-fed rivers in
276 central Europe while those for rivers with significant snow dynamics are good (Alps).
277 However, the annual cycle is more poorly reproduced in basins with strong soil freezing
278 dynamics (northern Fennoscandia) or strong damping of discharge amplitudes by large
279 lakes (southern Finland).

280

281 Perhaps more relevant in the present context is the model’s capability to reproduce inter-
282 annual variations in discharge. On average across 22 discharge stations, the standard
283 deviation of simulated annual discharge was 9% higher than observed and the spatial
284 correlation coefficient between the two 0.94. Like most models, VIC is better in
285 simulating high flows (95 percentile: Q95) than low flows (Q5); the first is slightly
286 overestimated, the second more seriously underestimated. The inter-annual variation in
287 Q5 is overestimated in central Europe and the Alps, but underestimated in Fennoscandia
288 (overall spatial correlation coefficient across Europe 0.40). The inter-annual variation
289 in Q95 shows no clear spatial pattern and the overall spatial correlation coefficient is
290 0.70.

291

292 All validation results discussed in these two paragraphs are for the VIC model forced
293 by E-OBS (v9, Haylock et al. 2008). Our forcing, WFDEI, shows higher precipitation
294 (+104 mm/yr) across most of Europe, except for the Alps, Scotland and westernmost
295 Norway. According to Greuell et al. (2015) this leads to higher mean discharge, higher
296 inter annual variability and higher Q95 (but not Q5) of simulated discharge for almost
297 all stations.

298

299

300 **2.2 Discharge observations**

301

302 For the assessment of skill with real discharge observations, two data sets with daily
303 resolution were acquired from the Global Runoff Data Centre, 56068 Koblenz, Germany
304 (GRDC): the GRDC data set and the European Water Archive (EWA) data set. We
305 mapped these two station data sets onto the VIC grid with its resolution of $0.5^\circ \times 0.5^\circ$
306 and aggregated the daily data at a time step of a month. To enable the investigation of
307 the effect of basin size on some of our results, we made two sub-classes of observations.
308 The first comprised observations for basins larger than 9900 km^2 (“large basins”), the
309 second contained basins smaller than the area of the grid cells, i.e. smaller than about
310 2530 km^2 in southern Europe (at 35° N) and 1050 km^2 at 70° N (“small basins”).

311

312 Initially, in many cases the location of observation stations did not match with the
313 corresponding river in the digital river network used in the routing calculations
314 (DDM30, see Döll and Lehner, 2002). We corrected for this issue by matching the
315 observations with the simulations by means of basin size. The size of the model basins
316 (“model basin area”) was determined by the DDM30 network. The size of the basins
317 upstream of the observation stations (“station basin area”) was taken from the meta data
318 of the observations. First the station basin area was compared to the model basin area of
319 the cell that is nearest to the station (“nearest model cell basin area”). After this first step
320 the mapping procedure for each observation differed between the two classes of basins.

321

322 For large basins we proceeded as follows:

- 323 - If the station and the nearest model cell basin area differed by less than 15%, the
324 observations were matched with the model calculations for the nearest model cell.
- 325 - Otherwise, the station basin area was compared with the model basin area of the
326 eight cells surrounding the nearest model cell.
- 327 - The minimum of the eight differences was determined.
- 328 - If that minimum was less than 15%, the simulations for the corresponding cell were
329 matched with the observations.
- 330 - Otherwise, the station was discarded.

331

332 For small basins we proceeded as follows:

- 333 - If the nearest model cell did not have an influx from any of the neighbouring cells,
334 its simulations were matched with the observations.
- 335 - Otherwise, all of the eight neighbouring cells without influx were selected.
- 336 - Their simulations were averaged and matched with the observations.

337

338 We further discarded all observations with less than 21 years of data within the
339 simulation period (1981-2010) for any of the months of the year. The final data set
340 within our European domain contained 111 cells with observations for large basins and
341 636 cells with observations for basins smaller than a model grid cell.

342

343 These data sets do not include any variable or parameter characterising the level of
344 human impact. To enable analysis of the effect of anthropogenic flow modifications on
345 predictive skill, we quantified the human impact by performing two model simulations
346 with the Lund-Potsdam-Jena managed Land (LPJmL) model (Rost et al., 2008;
347 Schaphoff et al., 2013). This model was operated at the same spatial resolution ($0.5^\circ \times$
348 0.5°) and with the same river network (DDM30) as VIC, but LPJmL does include dams
349 (GRanD database; Lehner et al., 2011) and associated reservoir management. From the
350 discharge output of a naturalized LPJmL run and an LPJmL run with reservoir operation
351 and irrigation, the human impact at cell level was quantified by computing the so-called
352 Amended Annual Proportional Flow Deviator (AAPFD; see Marchant and Hehir, 2002).
353 For the analysis in Sect. 3.3, we selected all discharge observations for large basins with
354 an AAPFD < 0.3 , i.e. basins with a relatively small degree of human impact (about half
355 of all 111 basins).

356

357

358 **2.3 Methods of analysis**

359

360 From the model output, consisting of daily means, monthly mean values were computed,
361 which were then used for the analysis. The analysis is restricted to runoff, defined here
362 as the amount of water leaving the model soil either along the surface or at the bottom,
363 and discharge, defined here as the flow of water through the largest river in each grid
364 cell. Discharge accumulates all runoff from cells that are upstream in the model river
365 network, with delays due to transport inside cells and through the river network. Hence,
366 whereas runoff represents only local hydrological processes, discharge aggregates
367 hydrological processes occurring in the entire basin upstream of a particular cell.

368

369 Instead of analysing skill per target season and/or for a number of consecutive lead
370 months, we analysed skill for every combination of the 12 target and the 7 lead months.
371 The thus achieved higher temporal resolution of the skill metrics enables a more
372 accurate determination of the beginning and end of periods of skill. Moreover, skill at a
373 monthly resolution provides the possibility to determine the consistency of the skill
374 where we define consistent skill as skill that persists during at least two consecutive
375 target or lead months. In accordance with Hagedorn et al. (2005) we designated the first
376 month of the hindcasts as lead month zero, so target month number is equal to the
377 number of the month of initialisation plus the lead month number.

378

379 Three skill metrics (see Mason and Stephensen, 2008, for a good discussion of the why
380 and how of these) were computed for each target and lead month separately: i) the
381 correlation coefficient between the observations and the *median* values of the hindcasts
382 (referred to as “correlation coefficient” or R), ii) the area beneath the Relative Operating
383 Characteristics (ROC) curve (shortly “ROC area”) and iii) the Ranked Probability Skill
384 Score (RPSS). The ROC area is computed for three categories of the observations and
385 hindcasts with an equal number of values, namely the categories containing the one third

386 highest, lowest and the remaining values (upper, lower and middle tercile, resp.; above,
387 below and near-normal, AN, BN and NN categories). The same subdivision of
388 observations and hindcasts in terciles was made to compute the RPSS. Since none of
389 these metrics is sensitive to systematic biases in the forecasting system, no attempt was
390 made to correct simulated runoff or discharge for any such errors prior to computing the
391 skill metrics. So we focus our evaluation on the models capability to predict river flow
392 anomalies rather than absolute river flows.

393

394 All three skill metrics quantify, though in different ways, how well the ranking of the
395 hindcasts matches the ranking of the observations. The correlation coefficient is a
396 measure of the association between (pseudo-) observation and forecast ensemble
397 median; we used the Pearson correlation coefficient. The ROC area is a measure of
398 resolution or discrimination and indicates whether the forecast probability of an event
399 (i.e. value falling in the considered tercile) is higher when such an event occurs
400 compared to when not. The RPSS is a measure of accuracy and summarizes in a single
401 number the skill of a forecast system to make forecasts with the correct percentage of
402 ensemble members falling in any of the defined terciles. Perfect forecasts have values
403 of 1 for all three skill metrics. Climatological forecasts (probabilistic forecasts that in
404 our case each year predict a 1/3 chance of a high or low anomaly occurring) lead to
405 values of 0 for R, 0.5 for the ROC area and 0 for the RPSS. In the computation of
406 significance of the RPSS, sampling errors, i.e. the limited number of ensemble members,
407 constitute a problem. They cause a bias in the RPSS when climatology is used as
408 reference (Mason and Stephenson, 2008). Therefore, the reference for the calculation of
409 the RPSS was generated by sampling randomly from the multinomial distribution with
410 $p = (1/3, 1/3, 1/3)$ and $N = 15$ (the number of ensemble members). In the present paper
411 each metric is designated as significant for p-values less than 0.05. For a data set of 30
412 years, this implies R is significant for values > 0.31 , ROC area for values > 0.69 and
413 RPSS for values that vary depending on the outcome of the random draw for the
414 reference. We checked these procedures to determine significance by analysing
415 hindcasts that have no skill. Such hindcasts indeed produced for all metrics a fraction of
416 cells with significant skill near the expected value of 0.05 (the p-value), indicating that
417 the procedures are correct.

418

419 To a large extent, we found that our results and conclusions, in terms of spatio temporal
420 patterns of skill, are independent of the chosen metric. Hence, and because among the
421 three metrics the correlation coefficient is the easiest to understand, we will discuss
422 results mostly in terms of the correlation coefficient, which is in line with Doblus-Reyes
423 et al. (2013). The sensitivity to the chosen metric and significant differences between
424 these metrics will be discussed in Sect. 4.2.

425

426 All metrics were computed using the low and high level R packages “SpecsVerification”
427 (Siegert et al., 2014) and “easyVerification” (Bhend et al., 2016), respectively. Metrics
428 cannot be computed (because they become ill-defined) if observations or hindcasts
429 within the entire 30 year period consist for more than one third of zeros or one sixth of

430 ties (i.e. equal values). Such skill gaps (i.e. the white terrestrial cells in Fig. 2 and 3)
431 mainly occur in the far North due to rivers that are frozen for at least a month in winter.

432

433

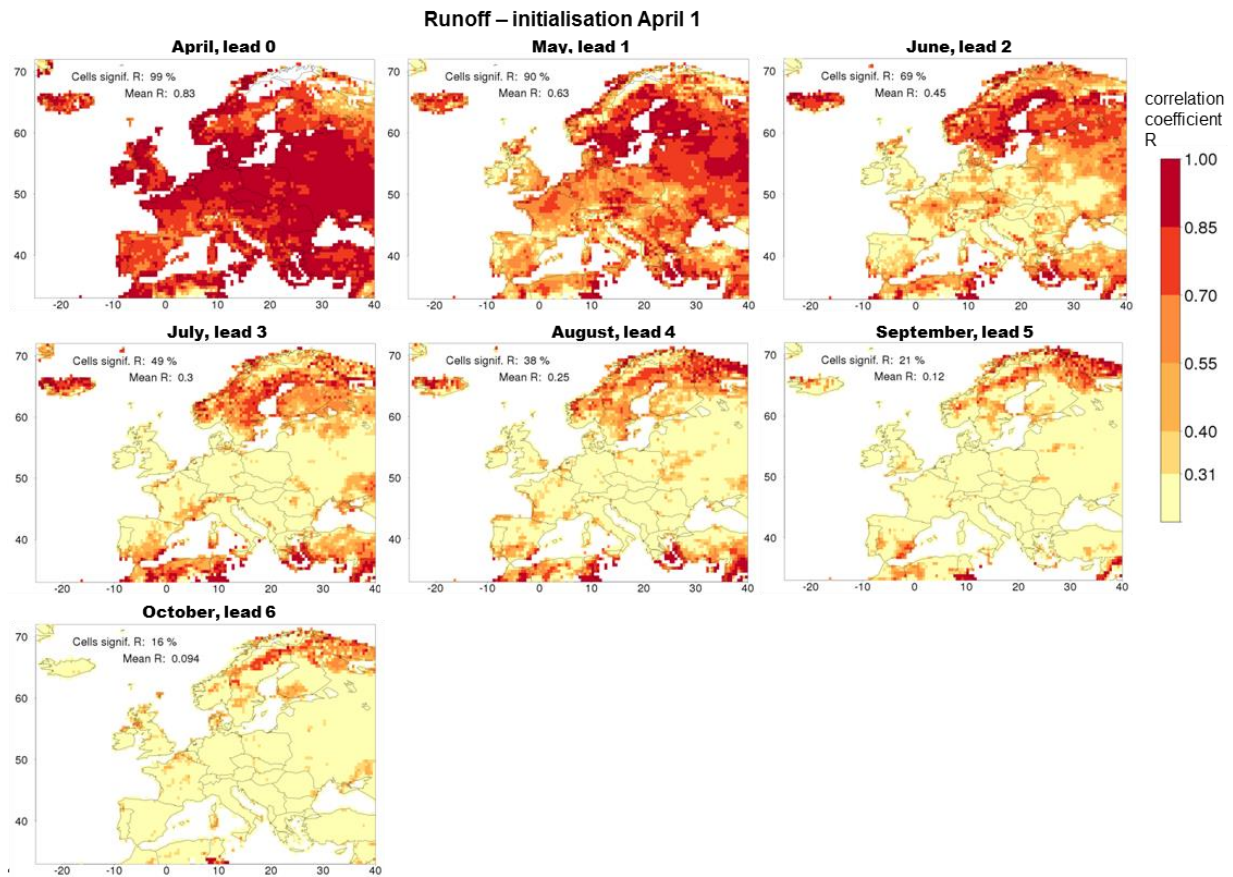
434 **3 Results**

435

436 **3.1 Spatiotemporal variation of skill in runoff forecasts**

437

438 Eighty-four maps of the skill of the runoff hindcasts were produced for all 12
439 initialisation months and all 7 lead months (all are presented in supplementary material
440 Fig. S1). Two cross-cuts through that collection are shown in Fig. 2 (for a single
441 initialisation month) and 3 (for a single lead month). The seven panels of Fig. 2 show
442 the skill of the hindcasts initialised on April 1 as a function of lead time. Cells with an
443 insignificant amount of skill are tinted yellow; cells where no metric could be computed
444 remain white. In lead month 0, significant skill is found across almost the entire domain
445 (99% of the cells). After the first lead month, the fraction of cells with significant skill
446 gradually decreases to reach 16% at the longest lead time (lead month 6). This is more
447 than expected for the case of completely unskilful simulations (5% of the cells), so at
448 the end of the hindcast simulations significant skill that does not occur due to chance is
449 still present in some regions. The general impression is that the pattern of skill does not
450 move in space but that skill is fading, i.e. for individual grid cells R is mostly decreasing
451 with increasing lead time. The same holds for initialisation in other months (see Fig. S1
452 in the supplementary material), with important exceptions better identified with Fig. 5
453 and discussed there.

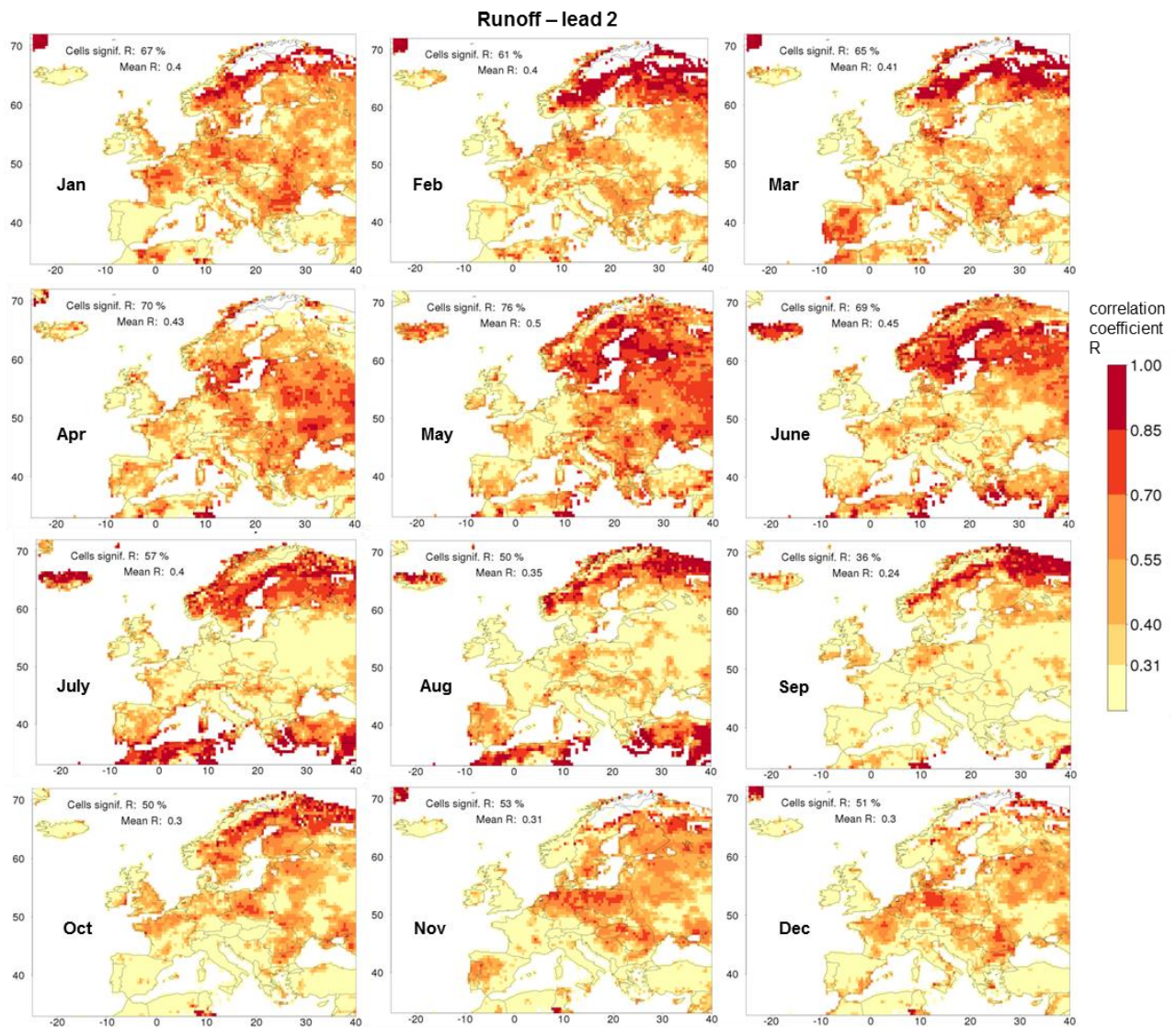


455

456 Figure 2: The skill of the runoff hindcasts initialised on April 1 for all seven lead
 457 months. The skill is measured in terms of the Pearson correlation coefficient
 458 between the median of the hindcasts and the observations (R). The threshold
 459 of significant skill lies at 0.31, so yellow cells have insignificant skill while
 460 darker cells have significant skill. White, terrestrial cells correspond to cells
 461 where observations or hindcasts consist for more than one third of zeros or
 462 one sixth of ties. The legend provides the fraction of cells with significant
 463 values of R (at the 5% level) and the domain-averaged value of R.

464

465



467

468 Figure 3: Annual cycle of skill (R) of runoff hindcasts for 12 target months, initialised
 469 at the beginning of the second month before (lead month 2). More
 470 explanation is given in the caption of Fig. 2.

471

472

473 The twelve panels of Fig. 3 show the annual cycle of the skill of the hindcasts for lead
 474 month 2, which is selected (also in Figures 6, 7 and 9) because at that lead time
 475 approximately 50% of the cells have significant skill. Consistent skill (persistent during
 476 at least 2 consecutive target months) is found in (causes of skill are reproduced here
 477 from the companion paper, Greuell et al., 2016):

478

- 478 - Fennoscandia. Much skill is present during the entire year, except for target months
 479 November and December, and there is a dip in the skill in April. Most of the skill
 480 is due to initial conditions of soil moisture. On average across the entire region, the
 481 skill reaches a maximum in May and June, i.e. at the end of the melting season,
 482 which is, as shown in the companion paper, largely due to initialising snow.
 483 Compared to the rest of the peninsula, there is generally less skill along the

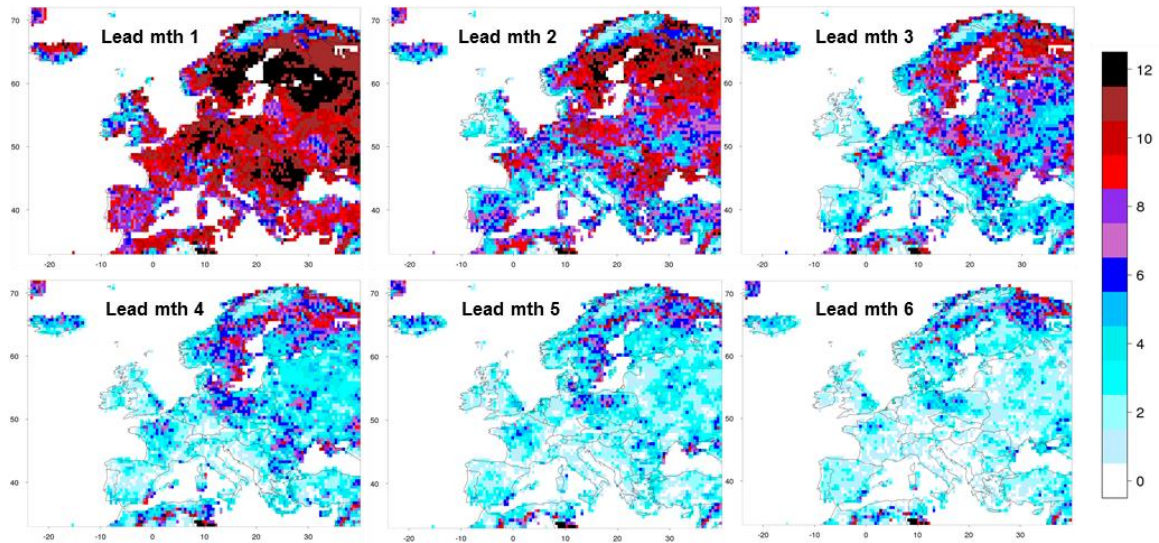
- 484 Scandinavian Mountain range. The companion paper shows some evidence that this
485 may be due to high variability of orographic rain, ill-represented in the S4 hindcasts.
- 486 - Poland and northern Germany. The core period lasts from November to January,
487 but it is extended with periods of less skill into October and the months from
488 February to May. Here the initialisation of soil moisture is the dominant cause of
489 skill. Snow initialisation contributes in April and May.
 - 490 - Western France, more or less from Paris to Brittany and roughly from December to
491 May. Skill derives from the initialisation of soil moisture.
 - 492 - The eastern side of Great Britain from January to April. Also here the skill derives
493 from soil moisture initialisation.
 - 494 - Romania and Bulgaria. The core as well as the whole period are the same as that
495 for Poland and northern Germany.
 - 496 - The southern part of the Mediterranean region from June to August. The high
497 amounts of skill are limited to the coastal parts of northern Africa, Sicily, southern
498 Greece, Turkey, Syria and Lebanon. This skill is due to initialisation of soil
499 moisture.
 - 500 - The Iberian peninsula in March and August with smaller amounts of skill in months
501 in between. The skill derives mainly from soil moisture in the initialisation. In
502 March there is a minor contribution from skill in the forecasts of precipitation.

503

504 From Fig. S1 we broadly conclude that regions with skill for lead month 2 retain their
505 skill for other (longer) lead times, but that the magnitude of skill decreases with
506 increasing lead time as demonstrated in Fig. 2 (keep in mind that a change in lead time
507 corresponds to a change in target time by the same amount). To give an example: for
508 lead month 3 patterns in the skill maps look similar to those provided in Fig. 3 but
509 colours are fainter and target months shift by one month ahead. There are many
510 exceptions to this general rule, e.g. skill due to snow melt that suddenly appears at the
511 end of the melt season at longer lead times while it was not present during the lead
512 months before (see Fig. 5 and the companion paper). A more detailed regional analysis
513 of some of these features is left for future case studies.

514

515



516

517

518 Figure 4: Number of months in a year with significant skill (R) in the runoff
519 forecasts of lead months 1-6.

520

521

522 Figure 4 displays a synthesis in the form of a six maps with the number of the 12 months
523 of the year with significant skill for lead months from 1 to 6. In accordance with what
524 was also illustrated by Fig. 2, the amount of significant skill degrades with increasing
525 lead time. There is generally more skill all over the year towards the north and the
526 northeast. Many of the regions with very little or no skill are coastal regions (e.g.
527 northern coast of Spain), especially coastal regions on the western side of land masses
528 (e.g. western coasts of Denmark, southern Norway, Italy, Croatia and the British Isles),
529 and mountain regions (e.g. the Alps except for its southern fringe, mountains in northern
530 Norway and Sweden and the Tatra on the border of Poland and Slovakia). The British
531 Isles exhibit little skill, except for the eastern coast of Great Britain in late winter and
532 early spring (JFMA). Many of the regions that were listed before as having consistent
533 skill for lead month 2 also appear as foci of skill during the whole year, namely
534 Fennoscandia, northeast Germany and northwest Poland, Romania and Bulgaria,
535 Western France and the eastern side of Great Britain. The companion paper shows that
536 for regions with skill during a large part of the year, this skill is due to initial conditions
537 of snow and/or soil moisture.

538

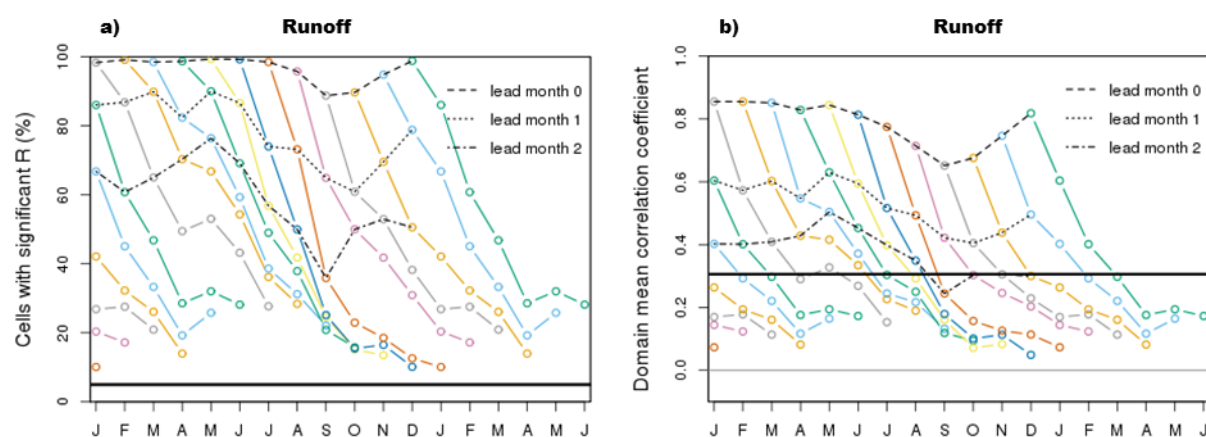
539 These pan-European results can be compared to those of Bierkens and Van Beek (2009).
540 They found maxima in predictability of winter discharge in Northern Sweden, Finland,
541 the region between Moscow and the Baltic Sea, Romania and Bulgaria, and Eastern
542 Spain. For the winter there is crude agreement with the current study about Northern
543 Sweden, Romania and Bulgaria, but not about the other regions. For the summer,
544 Bierkens and Van Beek (2009) compute maxima in skill for Southern Spain, Sardinia,
545 Western Turkey and South-western Finland, a pattern that broadly agrees with the

546 locations of the summertime maxima in skill we find (most of Fennoscandia and
 547 southern part of the Mediterranean region).

548

549 Singla et al. (2012) found considerable skill in the Seine basin for low flows from June
 550 – September, a bit more eastern from the region where we found skill. Trigo et al. (2004)
 551 using a statistical model based on December NAO indices found skill for JFM discharge
 552 (and hydropower production) for the Douro, Tejo and Guadiana basins covering most
 553 of central and western Iberia. We confirm this skill for March in these regions, but not
 554 for January and February while we find some skill for later months (March until
 555 August). Svensson et al. (2015) using a statistical model, based on NAO indices and
 556 river flow persistence, found good skill for winter river flows on the eastern side of the
 557 British Isles, consistent with our findings, and low but just significant skill along its
 558 western coast, which we do not reproduce.

559



560

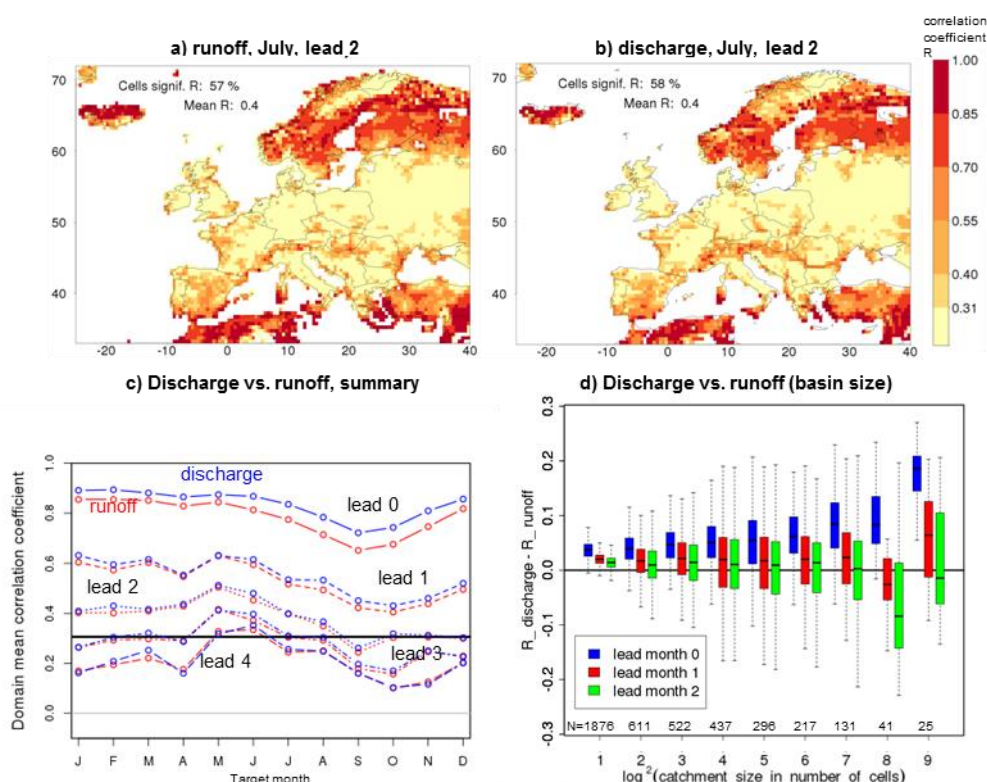
561 Figure 5: a) Fraction of cells with significant skill (in terms of R), and b) domain
 562 average correlation in the runoff hindcasts, as a function of initialisation
 563 month and lead time. Each coloured curve corresponds to the hindcasts
 564 initialised in a single month. For better visualisation, parts of the curves that
 565 end in the next year are shown twice, namely at the left-hand and the right-
 566 hand side of the graph. Black lines (dashed, dotted and dashed-dotted)
 567 connect the results for identical lead times. The horizontal line in a) shows
 568 the expected fraction of cells with significant skill, in the case that the
 569 hindcasts have no skill at all (5%), and in b) the minimal magnitude of the
 570 correlation of a single cell for it to be statistically significant.

571

572

573 Fig. 5a summarizes skill across the domain in terms of the fraction of cells with
 574 significant R for all initialisation and lead months. Overall there is a considerable
 575 amount of significant skill, with a minimum roughly from August to November and a
 576 maximum in May. For lead month 2 the fraction of cells with significant skill varies
 577 between 36% (September) and 76% (May). In all of the 84 combinations of initialisation
 578 and lead month, the theoretical value of no skill at all (5%) is exceeded, implying that

579 there are (small) pockets of skill even at lead month six. Individual curves show that
 580 skill is lost with increasing lead time. The exception is formed by hindcasts starting in
 581 November, December and January which gain skill when they progress from April to
 582 May, a phenomenon caused by initial conditions of snow that takes longer or shorter to
 583 completely melt in (late) spring. For details, see the companion paper. Fig. 5b shows
 584 decay and gain trends of the domain-averaged R. It shows that a forecast initialised in
 585 February exhibits higher domain average skill into June (5 lead months) than one
 586 starting in July into September (2 lead months). Similar summary plots for the other
 587 skill metrics are presented in the Fig. S2 and discussed in Sect. 3.4.
 588



589
 590
 591
 592
 593
 594
 595
 596
 597
 598
 599
 600
 601
 602
 603
 604

Figure 6: Comparison of the performance of the hindcasts of discharge and runoff using the pseudo-observations for verification. The two maps display R for runoff (a) and discharge (b) for hindcasts initialised on May 1 and target month July (see further explanation in Fig. 1). Panel c depicts the annual cycle of the domain-averaged R for runoff (red) and discharge (blue) for lead months 0 to 4. The horizontal line at 0.31 is the threshold of significance for a single cell. Panel d is a box plot of the difference between R for discharge and runoff as a function of the basin size. Each bin i contains the results for all basins with a maximum of 2^i cells and more than $2^{(i-1)}$ cells, e.g. bin 4 is for all basins with a size from 10 to 16 cells. Boxes represent the interquartile range and the median; whiskers extend to minimum and maximum values found in the bin. All values are average differences over the twelve months of the year and results are shown for three different lead times. The values above the abscissa give the number of cells in each bin.

605
606
607

3.2 Spatiotemporal variation of skill in discharge forecasts

608 This sub-section compares the skill for discharge with the skill for runoff. The two maps
609 of Fig. 6, which depict the skill in runoff and discharge hindcasts for July as lead month
610 2, show a high degree of similarity in terms of the patterns and the magnitude of the
611 skill. The same holds for other target months and lead times (not shown). There are,
612 however, subtle differences because rivers aggregate the skill, or lack of skill, from the
613 whole upstream part of their basin. As a result, cells containing rivers with large basins
614 may contrast against adjacent cells if these contain rivers with a small, local basin.
615 Indeed, some downstream parts of large rivers stick out in the skill map for discharge,
616 but not in the skill map for runoff. An example in Fig. 6b are the reaches of the Danube
617 along the Romanian-Bulgarian border, which show more skill than local small rivers in
618 adjacent cells, because some upstream parts of the Danube have more skill than the
619 region around the Romanian-Bulgarian border. An example that demonstrates the
620 opposite is the downstream part of the Loire showing less skill than local small rivers,
621 because upstream parts of the Loire have less skill than small, local rivers in the
622 downstream part.

623

624 Domain summary statistics of skill also differ slightly between runoff and discharge.
625 Figure 6c compares the annual cycle of the skill in discharge with the skill in runoff at
626 five different lead times. Here we show the difference in the domain-averaged R instead
627 of the fraction of cells with a significant R because in lead month 0 that fraction is close
628 to one for both variables. In terms of the domain-averaged R, predictability is higher for
629 discharge than for runoff for the first lead month. On average over the 12 months of the
630 year, the difference is 0.049. We ascribe this result to the combined effect of the delay
631 between runoff and discharge, with variations in discharge being later in time than the
632 corresponding variations in runoff, and the general tendency of decreasing skill with
633 lead time. The curves for the different lead times in Fig. 6c show that the difference in
634 skill between the two variables gradually disappears with increasing lead time (an
635 annual average of 0.020 and 0.012 for lead months 1 and 2, respectively). This is
636 compatible with the given explanation for the difference and the fact that the rate with
637 which skill is lost gradually decreases with increasing lead time.

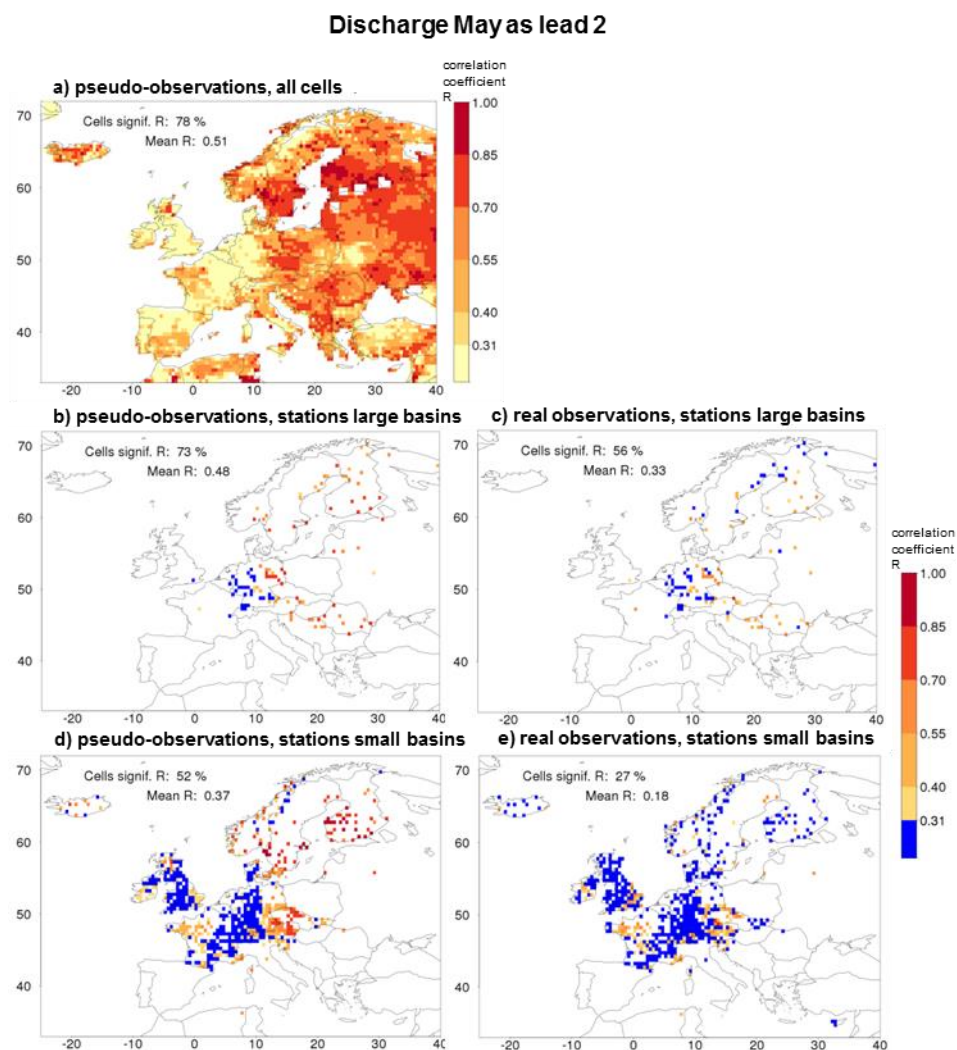
638

639 We finally analysed whether the difference in skill between discharge and runoff was a
640 function of the size of the basin (Fig. 6d). For the first lead month, when on average
641 there is more skill in discharge than in runoff, the difference increases with the size of
642 the basin. Again, this can be explained by the combination of the skill decaying with
643 time and the delay between runoff and discharge, with the delay increasing with the size
644 of the basin. For longer lead times (from lead month 1 on), when the domain-averaged
645 difference in skill has become very small, the figure shows no effect of the basin size.
646 Referring to the comparison between runoff and discharge in panels Fig. 6a and 6b for

647 lead month 2, cases like the Danube (more skill than local rivers) and the Loire (less
 648 skill than local rivers) tend to cancel when the entire domain and year are considered.
 649
 650

651 3.3 Verification of discharge with pseudo- and real observations

652
 653 So far, all skill was determined by using the discharge generated with the reference
 654 simulation. i.e. with pseudo-observations. In this section, this “theoretical skill” will be
 655 compared with the skill determined with real discharge as observed at gauging stations
 656 (“actual skill”) from the GRDC and EWA databases. Fig. 7 compares the theoretical
 657 skill (Fig. 7b and 7d for large and small basins, respectively) with actual skill (Fig. 7c
 658 and 7e for large and small basins, respectively) for a single combination of a target
 659 month (May) with a lead month (2). Small basins are defined as smaller than one $0.5^\circ \times$
 660 0.5° grid cell, large basins are larger than 9900 km^2 (see Sect. 2.2).
 661

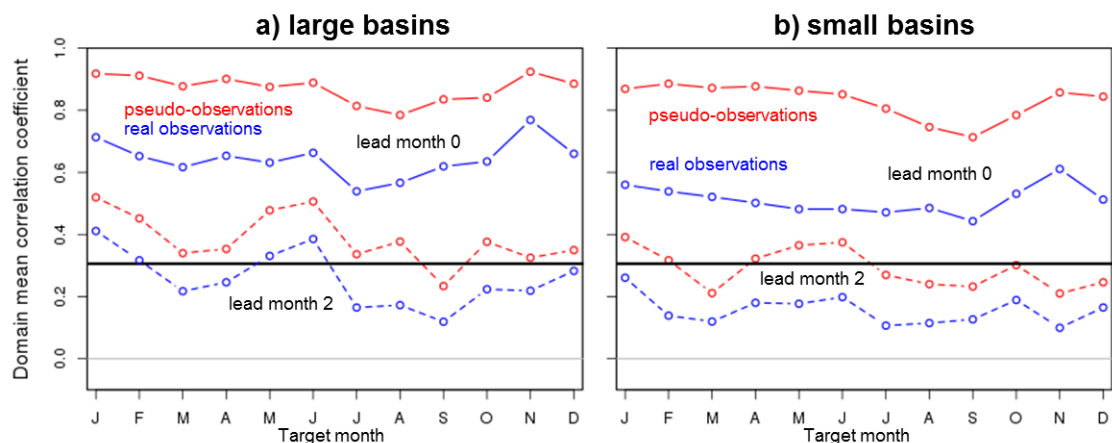


662
 663
 664 Figure 7: Skill (R) of the discharge hindcasts for May as lead month 2 (initialisation
 665 on March 1). In sequence: a) discharge verified with pseudo-observations,
 666 b) as a) but for cells with real observations representing large basins only,

667 c) discharge verified with real observations for large basins. Panels d) and
 668 e) are identical to b) and c), respectively, but for cells with real observations
 669 representing small basins. More explanation is given in the caption of Fig.
 670 1 but in panels d) and e) cells with insignificant skill are coloured blue
 671 instead of yellow for better contrast.
 672
 673

674 For this combination of May forecasts initialised in March, a substantial degradation in
 675 skill is found when the pseudo-observations are replaced by real observations. In terms
 676 of the fraction of cells with significant skill, the reduction is from 73 to 56 % for large
 677 basins and from 52 to 27 % for small basins and the domain-averaged R decreases from
 678 0.48 to 0.33 for large basins and from 0.37 to 0.18 for small basins. Especially the basins
 679 in northern Fennoscandia lose much of their skill when using actual instead of pseudo-
 680 observations. In this region VIC also performed poorly in reproducing historic flows.
 681 Specific discharge was underestimated and the annual cycle was poorly reproduced;
 682 especially the spring peak occurred too late and lasted too long (Greuell et al., 2015). In
 683 central Europe useful skill remains when using real observations, both for small and
 684 large basins. This is a region where VIC reproduced well annual cycles, though
 685 interannual variations in low flows were overestimated. For a few stations in Northwest
 686 France and Southeast England actual skill is larger than theoretical skill.
 687

688 Fig. 8 compares actual with theoretical skill for all target months and two lead times by
 689 considering the domain-mean R. Similar figures for the other skill metrics are presented
 690 in Fig. S4 and discussed in the next section. The reduction of actual relative to theoretical
 691 skill occurs for all combinations of target and lead months and does not exhibit a clear
 692 annual cycle. On average across all target months and for lead month 2, the ratio of
 693 actual to theoretical skill is 0.667 (0.258 divided by 0.387) for large basins and 0.538
 694 (0.156 divided by 0.290) for small basins. This is comparable to Van Dijk et al. (2013),
 695 who found a ratio of actual to theoretical skill of 0.54 for 6192 basins worldwide in
 696 terms of the ranked correlation coefficient.
 697



698

699

700 Figure 8: Comparison between verification of discharge with pseudo- (red) and real
701 (blue) observations in terms of the annual cycle of the domain mean R. The
702 horizontal line at 0.31 is the threshold of significance for a single cell.
703 Results are shown for cells representing large basins (left) and cells
704 representing small basins (right). Both panels depict cycles for lead months
705 0 and 2 only.
706
707

708 Comparing skill for small basins with skill for large basins in Fig. 8, we notice two
709 differences. Firstly, in terms of the domain mean R, theoretical skill is higher for large
710 basins than for small basins (0.39 and 0.29, respectively, for the annual mean and lead
711 month 2). However, this result holds for the cells with observations. If all cells of the
712 domain are considered, this difference becomes insignificantly small. So, the apparent
713 difference in theoretical skill between large and small basins can be attributed almost
714 entirely to the geographical distribution of the discharge monitoring stations, with
715 stations on small basins being relatively more often located in regions with relatively
716 little skill like Germany, France and the British Isles than large basin stations.
717

718 The second effect of the size of basins is that the ratio between theoretical and actual
719 skill is larger for small basins than for large basins, at least for lead month 0. This is
720 perhaps even more clear from Fig. S3 in the supplementary material. We speculate that
721 this is due to a combination of two effects. Firstly, there is more skill in simulations of
722 historic streamflow in large basins than in small basins (Van Dijk and Warren, 2010,
723 confirmed for VIC in Europe by Greuell et al. 2015). Secondly, as Van Dijk et al. (2013)
724 demonstrated, the ratio of actual to theoretical skill in the hindcasts is almost linearly
725 related to the skill of simulating historic streamflow. Combining these two relationships
726 confirms the relationship that we found, namely an increase in the ratio of actual to
727 theoretical skill with basin size.
728

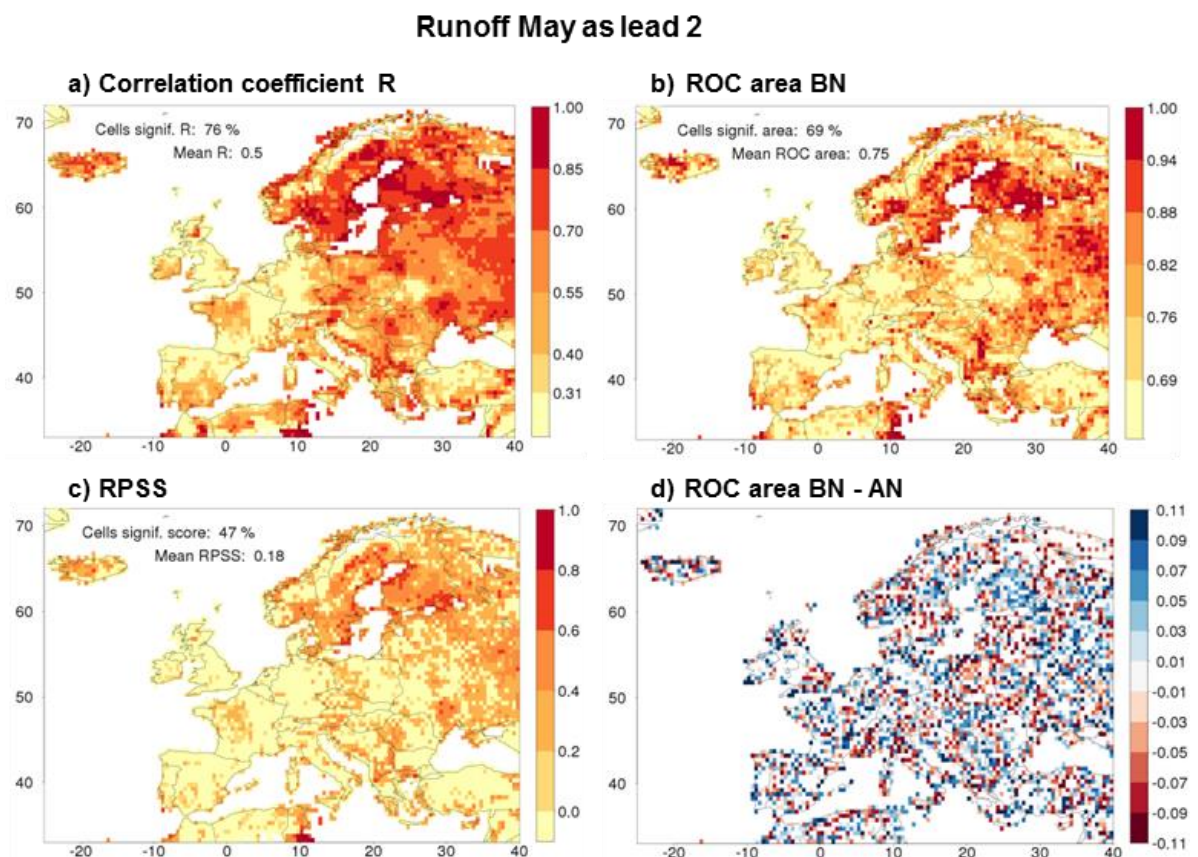
729 Finally, we investigated to what extent these results are affected by human interference,
730 keeping in mind that the simulations are naturalized, while the observations include
731 human impacts to a variable but unknown degree. Human interference is expected to
732 have a negative effect on actual skill and hence on the ratio of actual to theoretical skill.
733 For relatively natural "large basins" (AAPFD < 0.3; see end of Sect. 2.2), the ratio of
734 actual to theoretical skill was computed in terms of the domain mean R, averaged across
735 all target months and for lead month 2. We found a ratio of 0.686, which should be
736 compared to a ratio of 0.667 for the entire set of large basins (see above). So, as expected
737 the ratio is larger for basins with less impact. However, since the difference between the
738 two ratios is small we conclude that the effect of evaluating naturalised runs against
739 observations that are obviously affected by human interference, contributes only little
740 to the difference between actual and theoretical skill. A similar analysis was not applied
741 to the collection of small basins with observations, since these are smaller than the
742 spatial resolution of the simulations.
743

744
745
746
747
748
749
750
751
752
753
754
755
756
757
758
759
760
761
762
763
764
765
766

3.4 Results for other skill metrics

So far, skill was measured in terms of the correlation coefficient between the median of the hindcasts and the observations (R) only. This section compares those results, for runoff, with results in terms of other skill metrics. Fig. 9 gives an example for one particular target month and lead month, i.e. target May initialised in March (lead 2). Fig. 9a, 9b and 9c show the skill patterns for R, for the ROC area for Below Normal (BN) years and for the RPSS. The three patterns are spatially similar to a large degree, though the magnitudes and number of significant cells do differ. The pattern of the map of the ROC area for Above Normal (AN) years (see Fig. S1) is also similar to the patterns of the three maps shown. On average across all lead and target months, among cells that have significant R, 89% and 84% also have a significant ROC score for the BN tercile and the AN tercile, respectively, and 65% also have significant RPSS scores. The fraction of cells with no significant R, but with significant ROC or RPSS remains below the 5% level across all target and lead months.

The agreement that we find between the patterns of the different metrics is in accordance with a result mentioned in a global analysis of seasonal streamflow predictions by Van Dijk et al. (2013) who found high spatial correlation between the different skill metrics they used (among which R, the RPSS and the ranked correlation coefficient).



767

768 Figure 9: Maps of different skill metrics for one combination of a target month (May)
769 and a lead month (2) of the runoff hindcasts. Panels show a) R, b) the ROC
770 area for the below normal tercile, c) the Ranked Probability Skill Score
771 (RPSS) and d) the difference in ROC area between the BN and AN terciles.
772 In panels a), b) and c) skill is not significant in cells with a yellow colour.
773 Legends provide the fraction of cells with significant values of the metric
774 and the domain-averaged value of the metric.

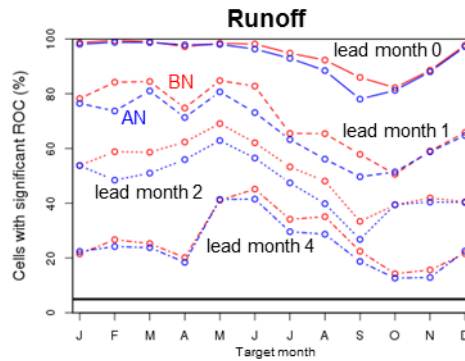
775
776
777 Although the different nature of the different metrics makes the interpretation of
778 quantitative differences between them difficult, this is not true for the ROC areas for the
779 different terciles. For the particular combination of May as target month and lead month
780 2 shown in Fig. 9, the domain-mean ROC area is largest for the BN tercile (0.75),
781 slightly smaller for the AN tercile (0.73) and much lower for the near-normal (NN)
782 tercile (0.58, see Fig. S2c and d). A similar tendency is found in the fraction of cells
783 with a significant ROC area (69%, 63% and 21%, respectively). In fact, in all
784 combinations of lead and target month the fraction of significant cells is larger for the
785 BN than for the AN tercile, as shown in Fig. 10. However, the AN and BN fractions of
786 cells tend to become equal (i) when they approach 1.0, (ii) when they approach the limit
787 of no skill (5%) and (iii) during target months from October to January. Finally, Fig. 9d
788 presents a map of the difference between the BN and the AN ROC area for May as lead
789 month 2. There is some organisation in the pattern but regions with a positive or a
790 negative difference between the two tend to be smaller than the regions with significant
791 skill in the maps of e.g. Figs. 2 and 3. Also, we did not detect much consistency, in the
792 sense of persistence during at least two consecutive target or lead months, in the patterns
793 of the difference between ROC AN and ROC BN.

794 In Fig. 9c the fraction of cells with a significant value of the RPSS is 47%, which is
795 somewhere between the fractions for ROC areas of the three terciles because the RPSS
796 represents the skill across all terciles.

797

798 For other combinations of target and lead months the results of this analysis are
799 qualitatively similar, see supplementary figures. All metrics show a minimum value in
800 the annual cycles in either September or in October, irrespective of lead time; maxima
801 are attained in February for lead month 0 shifting to May at longer lead times (Fig. S2).
802 We would finally like to note that, while in this sub-section we discussed runoff, we
803 made similar figures and calculations for discharge. Results for these two variables are
804 almost identical.

805



806
807

808 Figure 10: Skill of the runoff hindcasts in the Below Normal (BN) compared to the skill
809 of the runoff hindcasts in the Above Normal (AN) tercile. The plot depicts
810 annual cycles of the fraction of cells with a significant ROC area for the two
811 terciles and for four lead months.

812
813

814 4 Discussion

815

816 4.1 Theoretical versus actual skill

817

818 In the analysis of the differences between theoretical and actual skill, two essential
819 questions are: a) What are the conceptual differences between the physical systems that
820 generate the pseudo- and the real discharge observations, i.e. between the model
821 reference run and the real world. To answer this question, the components in the upper
822 and the lower box of the diagram in Fig. 1 need to be compared. b) What are the expected
823 effects of these differences on skill, i.e. on the comparison with the hindcasts. To answer
824 this question, the components that differ between the real world and the model reference
825 run need to be compared with the model hindcasts. The rule then is that skill decreases
826 with increasing disagreement between a component of the hindcast system and the
827 corresponding component of one of the other systems. The following components differ
828 between the real world and the model reference simulation:

829

- 830 1. Real meteorology differs from the meteorology assumed in the reference
831 simulation (WFDEI), both during the spin up period and during the hindcast
832 period. During spin up, model reference run and hindcasts have identical
833 meteorological forcing (WFDEI), which differs from real meteorology.
834 Therefore, this difference is expected to lead to more theoretical than actual skill.
835 During the hindcast period, all three systems have different meteorological
836 forcing. We do not have a well-founded expectation about any biases between
837 these three forcings and, hence, we have no expectation about its effect on the
838 difference between theoretical and actual skill. However, in Europe and beyond
839 the first lead month almost all skill in the seasonal forecasts is due to the initial
840 conditions (see the companion paper). Therefore, beyond the first lead month
841 and in Europe differences in forcing during the hindcast period have a negligible
effect on skill.

- 842 2. Models are imperfect, in terms of physics and in terms of spatial and temporal
843 discretisation, so model hydrology differs from real world hydrology. Hindcasts
844 and the pseudo-observations are produced with the same model, so
845 imperfections in model hydrology are expected to lead to more theoretical than
846 actual skill. One assumption implicitly made in the diagram is that the basin of
847 the observation station and the model basin are identical. This is not the case
848 (see Sect. 2.2), so differences between observation and model basin form an
849 additional cause of disagreements between theoretical and actual skill. Again,
850 this will favour theoretical skill with respect to actual skill since basins are
851 identical in the hindcasts and the reference simulation. In particular, differences
852 in meteorological forcing between the basin of the observation station and the
853 model basin might reduce actual skill. Van Dijk et al. (2013) investigated this
854 aspect by making simulations for Australia at different spatial resolutions and
855 verifying with networks of observations with different spatial densities. They
856 found that the resolution and perhaps the quality of the forcing data contributed
857 at least half to the difference between theoretical and actual skill.
- 858 3. In the real world discharge observations are subject to measurement errors.
859 Measurement errors of discharge are not constant over time (due to varying cross
860 sectional areas, following erosion and sedimentation) and therefore add noise to
861 the data; noise always reduces skill. There is no equivalent of this error in the
862 model environment. Hence, as for differences 1) and 2) this difference is
863 expected to lead to more theoretical than to actual skill.
- 864 4. Initial conditions are absent in this list of differences since they are not
865 independent components but entirely determined by two components of the
866 system listed above, namely meteorology and hydrology. Alternatively, initial
867 hydrological conditions could be taken from observations or by assimilation of
868 observations into model calculations. In that case, initial conditions would
869 become an independent or semi-dependent component of the system. However,
870 while model initial conditions would, of course, differ from real initial
871 conditions, the two model systems had identical initial conditions. Hence, this
872 difference would again be expected to lead to more theoretical than to actual
873 skill.

874

875 In summary, all of the conceptual differences between the generation of pseudo- and
876 real observations are expected to lead to more theoretical skill than actual skill, except
877 for the difference in meteorology during the hindcast period, which has, in the case of
878 Europe beyond the first lead month, a neutral effect, and otherwise an unknown effect.
879

880 Our data analysis, Sect. 3.3, broadly confirms that theoretical skill exceeds actual skill.
881 We also found cases where actual skill exceeds theoretical skill beyond lead month 0,
882 like for a few stations in Northwest France and Southeast England in Fig. 7. We ascribe
883 such cases to chance.

884

885 It is interesting to discuss what would happen in the utopian case that the system of the
886 model reference run would converge with the real world, i.e. if model meteorological
887 forcing and hydrology would approach perfection and if measurement errors would
888 approach zero. Equality of the two systems would, according to the analysis above, lead
889 to equality of theoretical and actual skill. However, we like to note that at the same time
890 optimisation of the model system can lead to a degradation of the theoretical skill due
891 to unrealistic memory time scales in the storage compartments of the hydrological
892 model before optimisation. If this memory, from stored water in either snow, soil or
893 aquifer is too strong, then skill will reduce with calibrating the model towards more
894 realistic storage accumulation. However, if this memory is too small before improving
895 the model, then, of course, the reverse would happen and skill increases with
896 optimisation.

897 An example proving this statement is a model that accumulates too much snow. The
898 model will do so both in the initial state of the reference simulation and the initial state
899 of the hindcasts and since more snow leads, at some stage of the melting season, to more
900 predictive skill, theoretical skill will be overestimated. A perfect model, accumulating
901 less but more realistic amounts of snow, would exhibit less skill. Another example is
902 predictive skill caused by interannual variations in the initial amount of soil moisture
903 and/or groundwater. A model that is imperfect because it overestimates the transport
904 speed of water through the soil and the groundwater reservoirs will do so both in the
905 reference simulation and the hindcasts. Predictive skill due to soil moisture initial
906 conditions will then occur too early. Compared to the model that overestimates transport
907 speed, a perfect model with smaller, realistic transport speed would yield less theoretical
908 skill at the early lead times.

909 Hence, theoretical skill is not equal to the maximum that could be accomplished if
910 hydrological model and meteorological forcing during the reference simulation were
911 perfect.

912 The version of VIC used in this study was calibrated by Nijssen et al. (2001) in a crude
913 way, in the sense that they assumed no spatial variation of the parameters set by
914 calibration within almost the entire European continent. Improving the calibration of
915 VIC would be an obvious candidate for trying to improve the seasonal predictions
916 discussed in this paper. This should lead to higher actual skill. However, the two
917 examples discussed above show that theoretical skill may actually, for certain locations,
918 months of initialisation and lead months, decline due to the recalibration.

919

920

921 **4.2 Results and uncertainties**

922

923 There seems to be a broad correspondence between the probabilistic forecast
924 verification presented here and the model validation presented in Greuell et al. (2015)
925 and Roudier et al. (2016). These studies found that average discharge and inter-annual
926 variations therein are well reproduced against observations, consistent with our result

927 that in the first lead month all skill scores, also against real observations (see Fig. S4 for
928 the lead 0 results), are good for large parts of Europe.

929

930 However, the relation between a model's ability to simulate historic streamflow and its
931 ability to generate skill in seasonal forecasts is complex. There is, for instance, no reason
932 to expect that regions with more theoretical skill than other regions would generally
933 correspond to regions with better historic streamflow simulations. Large model stores
934 of soil moisture and snow tend to lead to more theoretical skill, whether these stores are
935 realistic or not. If they are not realistic, simulations of historic streamflow will be poor,
936 despite the forecast skill. Another example of the problematic relation between
937 validation and verification is that, even in perfect models, regions with small model
938 stores of soil moisture and snow and regions with large interannual variation in
939 precipitation will exhibit small amounts of theoretical and actual skill. So, regions with
940 high quality historic streamflow simulations may for good reasons have little skill in the
941 forecasts.

942

943 However, what we would expect is that regions of poor model performance have little
944 actual skill (not necessarily little theoretical skill) in the forecasts. In our work, this
945 statement is broadly confirmed by the basins in northern Fennoscandia, which lose much
946 of their skill when using actual instead of pseudo-observations (Fig. 7). In this region
947 VIC indeed performed poorly in reproducing historic flows. Good model performance
948 probably is a necessary (but not sufficient) condition for the generation of actual skill in
949 seasonal forecasts. This is exemplified by some regions with considerable amounts of
950 actual skill in central Europe (e.g. northern part of the Balkans and the Elbe basin in Fig.
951 7), where VIC's simulations of historic streamflow are much better than in northern
952 Fennoscandia.

953

954 In a future extension of our work, an objective method like cluster analysis could reveal
955 regions where skill has a similar signature. This could lead to an improved assessment
956 of the physical and climatological factors that are responsible for the spatial variations
957 in skill found in this and its companion paper.

958

959 There also seems to be a broad correspondence between the regions and seasons with
960 skill identified in the present work and those identified in more spatially or temporally
961 confined studies based on entirely different physical or even statistical models. Without
962 repeating the more detailed description in the Introduction and the closer comparison in
963 Sect. 3.1, we restate here that the results of Bierkens and van Beek, (2009) and Thober
964 et al. (2015) were similar at the European domain. These pan-European studies, like
965 ours, confirm more regional studies such as for the British Isles (Svensson et al., 2015)
966 or France (Céron et al., 2010; Singla et al., 2012). Though a high resolution study like
967 the latter may add much spatial detail, this does not change the region and season of
968 skill.

969

970 Our results are based on a forcing with the 15 member, monthly initialized, 7 month
971 forecast version of ECMWF System 4, basically because at the start of this work that
972 hindcast was the only one accessible to us, but also because it allows verification at the
973 monthly resolution. Alternatively, we could have used the 51 member seasonally
974 initialised (4 times per year), 7 month forecast version of the same model. That would
975 have provided us with better constrained, more precise statistics (larger sample size), or
976 would have allowed assessment of more percentiles (e.g. quintiles instead of terciles) at
977 similar precision. However, the variation of skill over a year would not have been
978 resolved with such detail as in the present work. Finally, a 15 member, seasonally
979 initialized, 12 month forecast version of System 4 is available. Our results show that for
980 some regions at lead month 6 still a few, small pockets of consistent skill remain,
981 suggesting that extending the forecast for our domain might be worth exploring.

982
983 Other seasonal forecasting systems, based on different coupled ocean-climate models,
984 could have been used as meteorological forcing, such as CFSv2 (Saha et al., 2014) and
985 GloSea5 (MacLachlan et al., 2014). Given that, at least at large scales, multi model
986 ensembles exhibit better climate forecast skill than single models, it is interesting to
987 investigate if that additional skill also propagates into river flow forecasts. While this
988 seems to be true for the Eastern United States (Luo & Wood, 2008) it is not known if
989 similar conclusions could be drawn for Europe. A similar reasoning can also be extended
990 to the hydrological models: using a multi climate model ensemble to force a multi
991 hydrological model ensemble might also provide improved skill, as the latter models
992 may be complementary in the regions and seasons of best model performance. Bohn et
993 al. (2010) showed some advantage of using an ensemble of three hydrological models
994 (but with a single forcing), over using only the best of the three, but only after bias
995 correcting the hydrological output and making a linear combination of them with
996 monthly varying weights.

997

998

999 **4.3 Implications and recommendations**

1000

1001 Many conclusions drawn from this work are valid at the scale of our domain and not
1002 necessarily at the scale of river basins. Only in some parts of our analysis, especially
1003 where we focused on the annual cycle of the skill (Fig. 3), regional patterns at a scale
1004 smaller than that of the domain were discussed. This was done in a qualitative way.

1005

1006 For applications of these seasonal forecasts in decision making processes at (sub) basin
1007 level, a more detailed skill analysis is recommended for that specific (sub) basin,
1008 preferably after a better model calibration for that same basin. The facts presented in
1009 this study that anomaly correlations and ROC scores for the AN and BN terciles are
1010 significant for large parts of the domain for lead times up to several months, supported
1011 by (fairly) positive validation results for VIC (Greuell et al., 2015; Roudier et al. 2016),
1012 suggest these anomaly forecasts are good enough to be used as such. However, areas of
1013 significant RPSS are much smaller and remain significant for shorter lead times.

1014 Spatially distributed calibration of VIC model parameters, or distribution based
1015 calibration of modelled discharge to observations, or both, might also increase the
1016 RPSS. This might then allow forecasting of absolute discharge magnitudes and thus
1017 inform decision making processes that involve certain absolute discharge thresholds.

1018

1019 In Sect. 3 (Results) we already discussed the probable reasons for skill, which are much
1020 elaborated on in the companion paper. In general that paper shows that for most areas
1021 skill in runoff is caused by initialising snow and /or soil moisture properly, only in few
1022 areas and seasons skill in precipitation or skill in temperature and evapotranspiration
1023 adds to that beyond the first lead month. This has two implications: one is that, if ever
1024 the skill of seasonal climate forecasts improves for Europe, this may well translate to
1025 improved seasonal river flow forecast too. The second is that better initial conditions of
1026 snow water equivalent and soil moisture from observations may do the same, but the
1027 latter only if the spatial distribution of the soil moisture storage capacity is more realistic
1028 too (see Sect. 4.1).

1029

1030 Overall the present analysis shows that especially in winter, spring and early summer,
1031 there is potentially good skill to forecast runoff and discharge in large parts of Europe,
1032 with considerable lead time. While this broadly confirms previously published work,
1033 the present study (while being specific to our model setup) gives much more spatial and
1034 temporal (season and lead time) details. As such it provides a good basis to support
1035 operational forecasts and to add information about skill to seasonal forecasts, which is
1036 very important for proper value assessment and decision making.

1037

1038

1039 **5 Conclusions**

1040

1041 This paper is the first of two papers dealing with a model-based system built to produce
1042 seasonal hydrological forecasts (WUSHP: Wageningen University Seamless
1043 Hydrological Predictions). The present paper presents the development and the skill
1044 evaluation of the system for Europe, the companion paper provides an explanation of
1045 the skill or the lack thereof.

1046

1047 First, “theoretical skill” of the runoff hindcasts was determined using the output of the
1048 reference simulation as “pseudo-observations”. Using the correlation coefficient (R) as
1049 metric, hot spots of significant skill were found in Fennoscandia (from January to
1050 October), the southern part of the Mediterranean (from June to August), Poland,
1051 northern Germany, Romania and Bulgaria (mainly from November to January) and
1052 western France (from December to May). There is very little or no significant skill all
1053 over the year in some coastal and mountainous regions. The entire British Isles exhibit
1054 very little skill, except for the eastern coast of Great Britain. If the entire domain is
1055 considered, the annual cycle of skill has a minimum roughly from August to November
1056 and a maximum in May.

1057

1058 Runoff and discharge show a high degree of similarity in terms of the spatial patterns
1059 and the magnitude of the skill. However, when averaged over the domain and the year,
1060 predictability is slightly higher for discharge than for runoff for the first lead month (by
1061 0.049 in terms of R), but the difference decreases with increasing lead time. We also
1062 found that for lead month 0 the difference between discharge and runoff skill increases
1063 with the size of the basin.

1064

1065 Theoretical skill as determined with the pseudo-observations was compared to actual
1066 skill as determined with real discharge observations. On average across all target months
1067 and for lead month 2, skill reduction due to replacing pseudo- by real observations is
1068 larger for small basins than for large basins.

1069

1070 Spatio-temporal patterns for the different skill metrics considered in this study
1071 (correlation coefficient, ROC area and Ranked Probability Skill Score) are similar to a
1072 large degree. ROC areas tend to be slightly larger for the below normal than for the
1073 above normal tercile but not during target months from October to January.

1074

1075

1076 **6 Author Contributions**

1077

1078 Greuell and Hutjes designed the experiments, with suggestions from the other co-
1079 authors. Franssen and Greuell developed the workflow scripts and performed all the
1080 simulations. Greuell and Franssen developed the analyses and plotting scripts in R.
1081 Biemans did the LPJmL work on AAPFD. All co-authors participated in repeated
1082 discussions on interpretations of results and suggested ways forward in the analysis.
1083 Greuell prepared the first version of the manuscript with contributions from all co-
1084 authors. Hutjes and Greuell prepared revisions of the manuscript with contributions
1085 from all co-authors.

1086

1087

1088 **7 Conflicting Interests**

1089 The authors declare that they have no conflict of interest.

1090

1091

1092 **8 Acknowledgments**

1093 This study was financially supported by the EUPORIAS project (EUropean Provision
1094 of Regional Impact Assessment on Seasonal-to-decadal timescale); grant agreement No.
1095 308291, funded by the European Commission (EU) project in the Seventh Framework
1096 Programme. We thank the valued suggestions and insightful comments from two
1097 (anonymous) reviewers that contributed to an improved version of the manuscript.

1098

1099

1100 **9 References**

1101

- 1102 Alfieri, L., Pappenberger, F., Wetterhall, F., Haiden, T., Richardson, D., & Salamon, P.
1103 (2014). Evaluation of ensemble streamflow predictions in Europe. *Journal of*
1104 *Hydrology*, 517, 913-922.
- 1105 Bhend, J., Ripoldi, J., Mignani, C., Mahlstein, I., Hiller, R., Spirig, C., Liniger, M.,
1106 Weigel, A., Bedia Jimenez, J., De Felice, M., Siegert, S., (2016) easyVerification:
1107 Ensemble Forecast Verification for Large Data Sets. [https://CRAN.R-](https://CRAN.R-project.org/package=easyVerification)
1108 [project.org/package=easyVerification](https://CRAN.R-project.org/package=easyVerification)
- 1109 Bierkens, M. F. P., & Van Beek, L. P. H. (2009). Seasonal predictability of European
1110 discharge: NAO and hydrological response time. *Journal of Hydrometeorology*, 10(4),
1111 953-968.
- 1112 Bohn, T. J., Sonessa, M. Y., Lettenmaier, D. P. (2010). "Seasonal Hydrologic
1113 Forecasting: Do Multimodel Ensemble Averages Always Yield Improvements in
1114 Forecast Skill?" *Journal of Hydrometeorology* 11(6): 1358-1372.
- 1115 Bruno Soares, M. and S. Dessai (2016). Barriers and enablers to the use of seasonal
1116 climate forecasts amongst organisations in Europe. *Climatic Change* 137(1): 89-103.
- 1117 Céron, J. P., Tanguy, G., Franchistéguy, L., Martin, E., Regimbeau, F., Vidal, J. -P.
1118 (2010). "Hydrological seasonal forecast over France: feasibility and prospects."
1119 *Atmospheric Science Letters* 11(2): 78-82.
- 1120 Crochemore, L., Ramos, M. H. and Pappenberger, F. (2016). Bias correcting
1121 precipitation forecasts to improve the skill of seasonal streamflow forecasts. *Hydrol.*
1122 *Earth Syst. Sci.* 20(9): 3601-3618.
- 1123 Demirel, M.C., Booij, M.J. and Hoekstra, A.Y. (2015). The skill of seasonal ensemble
1124 low-flow forecasts in the Moselle River for three different hydrological models. *Hydrol.*
1125 *Earth Syst. Sci.*, 19, 275–291, 2015
- 1126 Doblas-Reyes, F. J., García-Serrano, J., Lienert, F., Biescas, A. P., & Rodrigues, L. R.
1127 (2013). Seasonal climate predictability and forecasting: status and prospects. *Wiley*
1128 *Interdisciplinary Reviews: Climate Change*, 4(4), 245-268.
- 1129 Döll, P., & Lehner, B. (2002). Validation of a new global 30-min drainage direction
1130 map. *Journal of Hydrology*, 258(1), 214-231.
- 1131 ECMWF Seasonal Forecast User Guide, retrieved from:
1132 [http://www.ecmwf.int/en/forecasts/documentation-and-support/long-range/seasonal-](http://www.ecmwf.int/en/forecasts/documentation-and-support/long-range/seasonal-forecast-documentation/user-guide/introduction)
1133 [forecast-documentation/user-guide/introduction](http://www.ecmwf.int/en/forecasts/documentation-and-support/long-range/seasonal-forecast-documentation/user-guide/introduction)
- 1134 Ghile, Y. B., & Schulze, R. E. (2008). Development of a framework for an integrated
1135 time-varying agrohydrological forecast system for Southern Africa: Initial results for
1136 seasonal forecasts. *Water SA*, 34(3), 315-322.

- 1137 Greuell, W., Andersson, J. C. M., Donnelly, C., Feyen, L., Gerten, D., Ludwig, F., and
1138 Schaphoff, S. (2015). Evaluation of five hydrological models across Europe and their
1139 suitability for making projections of climate change. *Hydrol. Earth Syst. Sci. Discuss.*,
1140 12, 10289-10330, doi: 10.5194/hessd-12-10289-2015
- 1141 Greuell, W., W. H. P. Franssen, H. Biemans and R. W. A. Hutjes. Seasonal streamflow
1142 forecasts for Europe – II. Explanation of the skill. (2016, in revision) to *Hydrol. Earth*
1143 *Syst. Sci.*, doi: 10.5194/hess-2016-604
- 1144 Hagedorn, R., Doblas-Reyes, F. J., & Palmer, T. N. (2005). The rationale behind the
1145 success of multi-model ensembles in seasonal forecasting–I. Basic concept. *Tellus A*,
1146 57(3), 219-233.
- 1147 Hamlet, A. F., Huppert, D., & Lettenmaier, D. P. (2002). Economic value of long-lead
1148 streamflow forecasts for Columbia River hydropower. *Journal of Water Resources*
1149 *Planning and Management*, 128(2), 91-101.
- 1150 Haylock, M. R., Hofstra, N., Klein Tank, A. M. G., Klok, E. J., Jones, P. D., & New, M.
1151 (2008). A European daily high-resolution gridded data set of surface temperature and
1152 precipitation for 1950–2006. *Journal of Geophysical Research: Atmospheres* (1984–
1153 2012), 113(D20).
- 1154 Juston, J., Jansson, P. E., & Gustafsson, D. (2014). Rating curve uncertainty and change
1155 detection in discharge time series: case study with 44-year historic data from the
1156 Nyangores River, Kenya. *Hydrological Processes*, 28(4), 2509-2523.
- 1157 Koster, R. D., Mahanama, S. P., Livneh, B., Lettenmaier, D. P., & Reichle, R. H. (2010).
1158 Skill in streamflow forecasts derived from large-scale estimates of soil moisture and
1159 snow. *Nature Geoscience*, 3(9), 613-616.
- 1160 Lehner, B., Reidy Liermann, C., Revenga, C., Vörösmarty, C., Fekete, B., Crouzet, P.,
1161 Döll, P., Endejan, M., Frenken, K., Magome, J., Nilsson, C., Robertson, J., Rödel, R.,
1162 Sindorf, N., Wissler, D. (2011): High resolution mapping of the world's reservoirs
1163 and dams for sustainable river flow management. *Frontiers in Ecology and the*
1164 *Environment* 9(9): 494–502.
1165
- 1166 Li, H., Luo, L. and Wood, E.F. (2008). Seasonal hydrologic predictions of low-flow
1167 conditions over eastern USA during the 2007 drought. *Atmospheric Science Letters*
1168 9(2): 61-66.
- 1169 Liang, X., Lettenmaier, D. P., Wood, E. F., & Burges, S. J. (1994). A simple
1170 hydrologically based model of land surface water and energy fluxes for general
1171 circulation models. *Journal of Geophysical Research: Atmospheres* (1984–2012),
1172 99(D7), 14415-14428.

- 1173 Luo, L. and E.F. Wood, 2008: Use of Bayesian Merging Techniques in a Multimodel
1174 Seasonal Hydrologic Ensemble Prediction System for the Eastern United States. *J.*
1175 *Hydrometeor.*, 9, 866–884, doi: 10.1175/2008JHM980.1
- 1176 MacLachlan, C., A. Arribas, K. A. Peterson, A. Maidens, D. Fereday, A. A. Scaife, M.
1177 Gordon, M. Vellinga, A. Williams, R. E. Comer, J. Camp, P. Xavier and G. Madec,
1178 2014. Global Seasonal forecast system version 5 (GloSea5): a high-resolution seasonal
1179 forecast system. *QJR Meteorol Soc*, doi:10.1002/qj.2396.
- 1180 Marchant, R., & Hehir, G. (2002). The use of AUSRIVAS predictive models to assess
1181 the response of lotic macroinvertebrates to dams in south-east Australia. *Freshwater*
1182 *Biology*, 47(5), 1033-1050.
- 1183 Mason, S. J., & Stephenson, D. B. (2008). How do we know whether seasonal climate
1184 forecasts are any good?. In *Seasonal Climate: Forecasting and Managing Risk* (pp. 259-
1185 289). Springer Netherlands.
- 1186 Mo, K. C., & Lettenmaier, D. P. (2014). Hydrologic prediction over the conterminous
1187 United States using the national multi-model ensemble. *Journal of Hydrometeorology*,
1188 15(4), 1457-1472.
- 1189 Molteni, F, Stockdale, T., Balmaseda, M., Balsamo, G., Buizza, R., Ferranti, L.,
1190 Magnusson, L., Mogensen, K., Palmer, T., Vitart, F. (2011). The new ECMWF seasonal
1191 forecast system (System 4). ECMWF Technical Memorandum 656.
- 1192 Mushtaq, S., Chen, C., Hafeez, M., Maroulis, J. and Gabriel, H., 2012: The economic
1193 value of improved agrometeorological information to irrigators amid climate variability.
1194 *Int. J. Climatol.*, 32, 567–581.
- 1195 Nijssen, B., O'Donnell, G. M., Lettenmaier, D. P., Lohmann, D., & Wood, E. F. (2001).
1196 Predicting the discharge of global rivers. *Journal of Climate*, 14(15), 3307-3323.
- 1197 Rost, S., Gerten, D., Bondeau, A., Lucht, W., Rohwer, J., & Schaphoff, S. (2008).
1198 Agricultural green and blue water consumption and its influence on the global water
1199 system. *Water Resources Research*, 44(9), doi 10.1029/2007WR006331.
- 1200 Roudier, P., Andersson, J.C.M., Donnelly, C., Feyen, L., Greuell, W. and Ludwig, F.,
1201 (2016). "Projections of future floods and hydrological droughts in Europe under a +2°C
1202 global warming." *Climatic Change* 135(2): 341-355.
- 1203 Saha, Suranjana and Coauthors, 2014: The NCEP Climate Forecast System Version 2
1204 *Journal of Climate* *J. Climate*, 27, 2185–2208. doi: 10.1175/JCLI-D-12-00823.1
- 1205 Schaphoff, S., Heyder, U., Ostberg, S., Gerten, D., Heinke, J., & Lucht, W. (2013).
1206 Contribution of permafrost soils to the global carbon budget. *Environmental Research*
1207 *Letters*, 8(1), 014026, doi:10.1088/1748-9326/8/1/014026.

- 1208 Sheffield, J., Wood, E. F., Chaney, N., Guan, K., Sadri, S., Yuan, X., and Ogallo, L.
1209 (2014). A drought monitoring and forecasting system for sub-Saharan African water
1210 resources and food security. *Bulletin of the American Meteorological Society*, 95(6),
1211 861-882.
- 1212 Shukla, S. and Lettenmaier, D. P. (2011). "Seasonal hydrologic prediction in the United
1213 States: understanding the role of initial hydrologic conditions and seasonal climate
1214 forecast skill." *Hydrol. Earth Syst. Sci.* 15(11): 3529-3538.
- 1215 Shukla, S., McNally, A., Husak, G., & Funk, C. (2014). A seasonal agricultural drought
1216 forecast system for food-insecure regions of East Africa. *Hydrology and Earth System
1217 Sciences*, 18(10), 3907-3921.
- 1218 Siegert, S., Bhend, J., Kroener, I., De Felice, M. (2014). SpecsVerification: Forecast
1219 Verification Routines for Ensemble Forecasts of Weather and Climate. [https://CRAN.R-
1220 project.org/package=SpecsVerification](https://CRAN.R-project.org/package=SpecsVerification)
- 1221 Singla, S., Céron, J. P., Martin, E., Regimbeau, F., Déqué, M., Habets, F., & Vidal, J.
1222 P. (2012). Predictability of soil moisture and river flows over France for the spring
1223 season. *Hydrology & Earth System Sciences*, 16: 201-216.
- 1224 Svensson, C., Brookshaw, A., Scaife, A. A., Bell, V. A., Mackay, J. D., Jackson, C. R.,
1225 Hannaford, J., Davies, H. N., Arribas A., Stanley, S. (2015). "Long-range forecasts of
1226 UK winter hydrology." *Environmental Research Letters* 10(6): 064006.
- 1227 Themeßl, M. J., Gobiet, A., & Leuprecht, A. (2011). Empirical-statistical downscaling
1228 and error correction of daily precipitation from regional climate models. *International
1229 Journal of Climatology*, 31(10), 1530-1544.
- 1230 Thober, S., Kumar, R., Sheffield, J., Mai, J., Schäfer, D., and Samaniegoet, L. (2015).
1231 "Seasonal Soil Moisture Drought Prediction over Europe Using the North American
1232 Multi-Model Ensemble (NMME)." *Journal of Hydrometeorology* 16(6): 2329-2344.
- 1233 Trigo, R. M., Pozo-Vázquez, D., Osborn, T.J., Castro-Díez, Y., Gámiz-Fortis, S.,
1234 Esteban-Parra, M.J. (2004). "North Atlantic oscillation influence on precipitation, river
1235 flow and water resources in the Iberian Peninsula." *International Journal of Climatology*
1236 24(8): 925-944.
- 1237 Van Dijk, A. I., Peña-Arancibia, J. L., Wood, E. F., Sheffield, J., & Beck, H. E. (2013).
1238 Global analysis of seasonal streamflow predictability using an ensemble prediction
1239 system and observations from 6192 small basins worldwide. *Water Resources Research*,
1240 49(5), 2729-2746.
- 1241 Van Dijk, A. I. J. M., and G. A. Warren (2010), AWRA Technical Report 4, Evaluation
1242 Against Observations, WIRADA/CSIROWater for a Healthy Country Flagship,
1243 Canberra. [http://www.clw.csiro.au/publications/waterforahealthycountry/2010/wfhc-
1244 awras-evaluationagainst-observations.pdf](http://www.clw.csiro.au/publications/waterforahealthycountry/2010/wfhc-awras-evaluationagainst-observations.pdf)

- 1245 Weedon, G. P., Balsamo, G., Bellouin, N., Gomes, S., Best, M. J., & Viterbo, P. (2014).
1246 The WFDEI meteorological forcing data set: WATCH Forcing Data methodology
1247 applied to ERA-Interim reanalysis data. *Water Resources Research*, 50(9), 7505-7514.
- 1248 Wood, A. W., & Lettenmaier, D. P. (2006). A test bed for new seasonal hydrologic
1249 forecasting approaches in the western United States. *Bulletin of the American*
1250 *Meteorological Society*, 87(12), 1699.
- 1251 Wood, A. W., Hopson, T., Newman, A., Brekke, L., Arnold, J. and Clark, M. (2016).
1252 Quantifying Streamflow Forecast Skill Elasticity to Initial Condition and Climate
1253 Prediction Skill. *Journal of Hydrometeorology* 17(2): 651-668.
- 1254 Yuan, X., Wood, E. F., Luo, L., & Pan, M. (2013). CFSv2-based seasonal hydroclimatic
1255 forecasts over the conterminous United States. *Journal of Climate*, 26, 4828-4847.
- 1256 Yuan, X., Wood, E. F., & Ma, Z. (2015). A review on climate-model-based seasonal
1257 hydrologic forecasting: physical understanding and system development. *Wiley*
1258 *Interdisciplinary Reviews: Water*, 2(5), 523-536.
- 1259